Received: 2 June 2023 | Revised: 21 December 2023 | Accepted: 2 January 2024

DOI: 10.1111/gcb.17153

Global Change Biology WILEY

REVIEW

Carbon sequestration in the subsoil and the time required to stabilize carbon for climate change mitigation

Carlos A. Sierra[1,2] | Bernhard Ahrens[1] | Martin A. Bolinder[2] | Maarten C. Braakhekke[3] | Sophie von Fromm[1,4] | Thomas Kätterer[2] | Zhongkui Luo[5] | Nargish Parvin[2] | Guocheng Wang[6]

[1]Max Planck Institute for Biogeochemistry, Jena, Germany

[2]Department of Ecology, Swedish University of Agricultural Sciences, Uppsala, Sweden

[3]Wageningen Environmental Research, Wageningen UR, Wageningen, The Netherlands

[4]Department of Environmental Science, ETH Zurich, Zurich, Switzerland

[5]College of Environmental and Resource Sciences, Zhejiang University, Hangzhou, China

[6]Faculty of Geographical Science, Beijing Normal University, Beijing, China

Correspondence
Carlos A. Sierra, Max Planck Institute for Biogeochemistry, Jena, Germany.
Email: csierra@bgc-jena.mpg.de

Funding information
Horizon 2020 Framework Programme, Grant/Award Number: 862695; Swedish University of Agricultural Sciences; Max Planck Society; International Max Planck Research School for Global Biogeochemical Cycles

Abstract

Soils store large quantities of carbon in the subsoil (below 0.2 m depth) that is generally old and believed to be stabilized over centuries to millennia, which suggests that subsoil carbon sequestration (CS) can be used as a strategy for climate change mitigation. In this article, we review the main biophysical processes that contribute to carbon storage in subsoil and the main mathematical models used to represent these processes. Our guiding objective is to review whether a process understanding of soil carbon movement in the vertical profile can help us to assess carbon storage and persistence at timescales relevant for climate change mitigation. Bioturbation, liquid phase transport, belowground carbon inputs, mineral association, and microbial activity are the main processes contributing to the formation of soil carbon profiles, and these processes are represented in models using the diffusion–advection–reaction paradigm. Based on simulation examples and measurements from carbon and radiocarbon profiles across biomes, we found that advective and diffusive transport may only play a secondary role in the formation of soil carbon profiles. The difference between vertical root inputs and decomposition seems to play a primary role in determining the shape of carbon change with depth. Using the transit time of carbon to assess the timescales of carbon storage of new inputs, we show that only small quantities of new carbon inputs travel through the profile and can be stabilized for time horizons longer than 50 years, implying that activities that promote CS in the subsoil must take into consideration the very small quantities that can be stabilized in the long term.

KEYWORDS
climate change mitigation, diffusion–advection–reaction, microbial decomposition, organic matter stabilization, radiocarbon, soil carbon sequestration, transit time

1 | INTRODUCTION

Soil carbon stocks below the topsoil (below 0.2 m depth) are not only one of the largest carbon (C) reservoir on the terrestrial surface but are also relatively old, as demonstrated by radiocarbon measurements (He et al., 2016; Heckman et al., 2022; Mathieu et al., 2015; Shi et al., 2020). These radiocarbon measurements along the vertical profile have shown that the age of carbon increases significantly with depth, indicating that carbon may be stabilized for centuries to millennia in the subsoil. It is therefore reasonable to think that soils could act as a large sink for fossil-fuel-derived carbon if subsoil carbon sequestration (CS) is promoted, particularly in agricultural and managed lands (Button et al., 2022; Rumpel et al., 2012).

The subsoil has a large influence on ecosystem productivity and the supply of ecosystem services. It has been estimated that between 10% and 80% of the nutrient and water requirement of plants are provided by the subsoil (Hinzmann et al., 2021). Carbon stored in subsoils generally contributes to more than half of the total stocks within a soil profile. However, the amount of organic C stored in soil varies among biomes; relative to the first meter, between 43% and 71% of soil organic carbon (SOC) is found at depths below 20 cm (Jobbágy & Jackson, 2000). In agricultural soils, the amount of SOC stored in subsoils (up to 1 m depth) is similar to that in the topsoil arable layer (Morari et al., 2019). Due to cost limitations and focus on productivity, studies in agroecosystems often consider only the arable layer (>90% observations), where most changes in soil C are assumed to occur because C cycling is more dynamic in topsoil compared to deeper soil layers (Bolinder et al., 2020). However, subsoil C is not insensitive to agricultural management practices. There is evidence from long-term field experiments that management practices affect C stocks at decadal timescales in the upper part of the subsoil or even deeper (e.g., Börjesson et al., 2018; Dal Ferro et al., 2020; Kätterer et al., 2014; Kirchmann et al., 2013; Menichetti et al., 2015; Slessarev et al., 2020).

Furthermore, effects on subsoil carbon are evident when comparing annual versus perennial crops with more well-developed root systems or versus other deep-rooting species (Carter & Gregorich, 2010; Collins et al., 2010; Guan et al., 2016; VandenBygaart et al., 2011). Major land-use changes, such as cropland to grassland or cropland to forest and vice versa, may also, in some cases, induce changes in subsoil carbon (Guo & Gifford, 2002; Poeplau & Don, 2013). Button et al. (2022) reviewed several other options than the traditional management practices for increasing subsoil C, such as burial of organic matter or biochar addition to the subsoil. There is a need for including subsoil carbon in model-based estimates of CS (Button et al., 2022; Hicks Pries et al., 2023), but the mechanisms governing the effect of changes in subsoil carbon are understudied, which has been identified as a major knowledge gap (Chenu et al., 2019; Lorenz & Lal, 2005) while raising awareness of the potential for subsoils to promote SOC sequestration (Chen et al., 2018; Kautz et al., 2013).

Indeed, the use of deep-rooting plant species has been suggested as a land management strategy to promote carbon input to subsoil and thus sequestering soil carbon and mitigating climate change in cropping systems (Kell, 2011; Thorup-Kristensen et al., 2020). However, there are mixed results regarding the time new carbon inputs to subsoil would be stabilized on decadal timescales. Recent quantifications of the transit time of carbon inputs across soil depth showed that carbon inputs transit fast in all soil layer depths, challenging the efficiency of promoting carbon inputs to subsoil for soil CS (Wang, Xiao, et al., 2023; Xiao et al., 2022).

Managing soils for C sequestration purposes implies that the fate and transit time of new carbon inputs can be accurately quantified (Crow & Sierra, 2022). Mathematical models of subsoil carbon dynamics play an important role for this purpose and can be used to estimate the amount and persistence of new carbon due to land management.

In this review, we survey the main processes that contribute to soil carbon storage and dynamics in the subsoil, with particular emphasis on mathematical models of subsoil carbon dynamics. Our guiding question is whether a process understanding of soil C movement through the vertical profile can help us to assess C storage and persistence at timescales relevant for climate change mitigation. For this purpose, we first review the process understanding of subsoil C dynamics and then review mathematical models used in the past to represent these processes. Based on this review, we show that most previous models can be generalized under one single modeling paradigm, and through examples, we show the main contribution of different processes in shaping soil carbon profiles. In addition, we present a conceptual framework to assess the fate of new carbon inputs as they move through the subsoil. We use the theoretical framework provided by the transit time distribution of carbon in compartmental systems (Metzler & Sierra, 2018; Sierra et al., 2017; Sierra, Hoyt, et al., 2018) and discuss our results in the context of soil carbon management for climate change mitigation.

2 | PROCESSES CONTRIBUTING TO THE FORMATION OF SOIL CARBON PROFILES

A number of physical, chemical, and biological processes contribute to the formation of soil carbon profiles, which have been reviewed with some detail elsewhere (e.g., Button et al., 2022; Hicks Pries et al., 2023). Here, we briefly review some of these processes, grouping them according to their most common representation in models. Our objective is to make a parallel between process understanding and mathematical representations in models, which are reviewed in Section 3.

2.1 | Pedoturbation as diffusive vertical movement

Processes that mix the soil are commonly referred to as pedoturbation (Fey & Schaetzl, 2017; Hole, 1961), which include the reworking activity of soil fauna (bioturbation), freezing and thawing cycles (cryoturbation) (Beer et al., 2022; Bockheim, 2007; Johnson et al., 1987),

uprooting of trees (Schaetzl et al., 1990), swelling and translocation of clays (Finke, 2012), and human disturbances such as tillage (Fey & Schaetzl, 2017; Keyvanshokouhi et al., 2019). Bioturbation and tillage are the pedoturbation processes most commonly considered in models of soil carbon profiles, mostly represented in analogy to particle diffusion.

Soil mixing by bioturbation has a homogenizing effect on soil properties: it increases dispersal of particles, reduces concentration gradients, and destroys layering (Johnson et al., 1987). Hence, bioturbation leads to organic matter diffusion and, potentially, to deepening of the soil profile. In croplands, tillage contributes to the vertical mixing of soil carbon, altering the depth distribution of root inputs and crop residues (Luo et al., 2010). Depending on ploughing depth, the effects of tillage may only concentrate on the topsoil and may be difficult to observe at depths below 40 cm (Keyvanshokouhi et al., 2019; Luo et al., 2010; Mary et al., 2020). Due to this mixing effect, both bioturbation and tillage are commonly represented in models as a process of particle diffusion.

2.2 | Advective transport in liquid phase

A small part of organic matter in soils is dissolved in the liquid phase. Concentrations of dissolved organic carbon (DOC) are typically so low that total organic carbon in solution is negligible compared to the immobile fraction (Michalzik et al., 2001). However, leaching and decomposition fluxes of dissolved organic matter may be important terms in shaping the dynamics of soil carbon at depth (Neff & Asner, 2001; Kalbitz & Kaiser, 2008; Kindler et al., 2011; Kaiser & Kalbitz, 2012). DOC is highly relevant for the formation of the soil profile since it is subject to potentially very fast transport with downward water fluxes and represents a mechanism of organic matter input at depths well below the zone where bioturbation and root input are relevant (Rumpel et al., 2012). Furthermore, adsorption of DOC to the mineral phase is one of the main mechanisms for organic carbon stabilization and persistence (Kalbitz & Kaiser, 2008).

The concentration of DOC in soils covaries with precipitation (Liu et al., 2021), as water acts as the main medium for DOC transport. Therefore, rates of vertical water movement are commonly used to estimate DOC vertical transfer as an advective process (Ota et al., 2013).

A considerable part of DOC is easily degradable, with low-molecular weight compounds decreasing strongly with depth (Roth et al., 2019). An important mechanism for DOC removal is immobilization due to interactions with the solid phase and (co-)precipitation. Through a range of chemical mechanisms, DOC is adsorbed to surfaces of minerals (particularly Al and Fe hydroxides and clay) and, to a lesser extent, to solid organic matter (Kalbitz & Kaiser, 2008; Neff & Asner, 2001).

One important characteristic of representing liquid-phase transport as an advective process is that carbon is moved to parts of the profile where decomposition is slow, preventing fast losses due to microbial activity.

In layers with high organic matter concentrations, an important additional transport flux occurs that is generally ignored in soil carbon profile models. Loss of mass due to decomposition leads to downward shift of material above, while surface litter deposition continually buries older material. This mass-loss causes advective downward or upward flow of material unrelated to mixing or water movement (Ahrens et al., 2015). Kaste et al. (2007) found this process to be relevant for the vertical distribution of 210Pbex in the organic surface horizon of a podzol, and Hilbert et al. (2000) for modeling subsidence of peat soils.

2.3 | Depth dependence of organic matter input

The relative distribution of litter input between above- and belowground fractions, as well as the vertical distribution of the belowground input, is highly relevant for the carbon profile. Jobbágy and Jackson (2000) found a significant relationship between vertical soil carbon distribution and plant functional type, which is partially explained by ecosystem-level root/shoot ratios and the vertical distribution of root biomass. Since net primary production (NPP) is the source of litter input, its partition between above- and belowground biomass is a good predictor of the relative proportions of aboveground litter fall and rhizodeposition (Raich & Nadelhoffer, 1989; Xiao et al., 2023).

Synthesizing global data sets, including NPP measurements from 725 soil profiles and root biomass and its depth distribution from 559 soil profiles, Xiao et al. (2023) recently mapped depth-resolved belowground NPP (BNPP) at 1 km resolution across the globe. They found that global average BNPP allocated to the 0–20 cm soil layer is estimated to be 1.1 $MgC\,ha^{-1}\,year^{-1}$, accounting for ~60% of total BNPP. Across the globe, the depth distribution of BNPP varies largely but mostly follows a decreasing trend with depth, and more BNPP is allocated to deeper layers in hotter and drier regions. The highest levels of BNPP and carbon inputs to subsoil are in tropical and subtropical latitudes, as well as in temperate forests and grasslands, while the lowest levels of BNPP are in desserts and high-latitude regions (Xiao et al., 2023).

In croplands, the belowground distribution of root inputs is associated with crop type and whether annual or perennial cropping systems are in place (Hicks Pries et al., 2023; Mosier et al., 2021). In a review for temperate agricultural crops, Fan et al. (2016) showed that 50% of the roots mostly accumulate in the upper 8–20 cm, and Bolinder et al. (2007) found that the proportion of total NPP allocated belowground for common agricultural crops and perennial forages represents about 20% and 50%, respectively.

Independent of vegetation or crop type, root distribution seems to be mostly determined by soil hydrology, as demonstrated by significant relationships between annual potential evapotranspiration, precipitation, and soil texture (Schenk & Jackson, 2002a). In more water-limited ecosystems, plants tend to have deeper root profiles to maximize water uptake (Schenk & Jackson, 2002b). Roots may also preferentially grow in the organic surface layer, if present,

due to the high nutrient and moisture availability there (Jordan & Escalante, 1980; Schenk & Jackson, 2002a).

2.4 | Depth dependence of decomposition and microbial activity

A distinct property of most soils is the decrease of radiocarbon (^{14}C) activity with depth, indicating a higher average age of carbon since plant uptake from the atmosphere and a decrease in decomposition rates with depth (He et al., 2016; Heckman et al., 2022; Hicks Pries et al., 2023; Lawrence et al., 2020; Mathieu et al., 2015; Rumpel & Kögel-Knabner, 2011; Scheibe et al., 2023). Potential factors responsible for this age gradient include (c.f. Ahrens et al., 2020): the slow downward transport of carbon fractions that are either very recalcitrant or recurrently recycled by microbes (Elzein & Balesdent, 1995; Gleixner, 2013; Kaiser & Kalbitz, 2012; Roth et al., 2019); decreasing microbial activity along the profile (Jenkinson & Coleman, 2008; Koven et al., 2013; Persson et al., 2000; Wang et al., 2021), and the increasing role of organo–mineral associations with depth (Cotrufo & Lavallee, 2022; Eusterhues et al., 2003; Georgiou et al., 2022; Hicks Pries et al., 2023; Rasmussen et al., 2018; Rumpel & Kögel-Knabner, 2011). The reason for this gradient is not fully understood yet and needs further exploration (Guo et al., 2023). It may be caused by the selective preservation of recalcitrant compounds combined with downward transport (Elzein & Balesdent, 1995; Luo et al., 2020) as well as nonlinear interactions among C fractions such as priming (Guenet et al., 2013; Liang et al., 2018; Wang et al., 2021).

A further cause of stabilization in deep soil is physical disconnection between microbes and substrates (Don et al., 2013; Gleixner, 2013). Most microbial activity in deep soils is located in so-called hot spots: root and earthworm channels and preferential water flow paths (e.g., cracks). Organic matter outside of these zones may be stabilized due to spatial separation from decomposers (Chabbi et al., 2009).

2.5 | Land management practices that affect soil C profiles

The distribution of C along the vertical profile can be modified by management practices on cropland, rangeland, and forest soils. Historically, the management and cultivation of soils have resulted in a significant carbon loss of about 133 PgC (Sanderman et al., 2017). Hicks Pries et al. (2023) categorize management practices that affect subsoil carbon in three groups: physical redistribution due to tillage, changes in the vertical distribution of root inputs due to vegetation change, and the addition of exogenous C inputs applied at the surface or buried at depth. These practices tend to modify the physical mixing of particles in soil, the transport of water and advective movement of C, and the vertical distribution of root inputs and microbial activity.

Practices that alter the physical structure of soils, such as tillage, constantly redistribute organic matter between top and subsoil, acting as a mechanism for the diffusion of organic and mineral-associated carbon particles (Button et al., 2022; Keyvanshokouhi et al., 2019; Mary et al., 2020). Deep ploughing (Alcántara et al., 2016; Wang, Xu, et al., 2023) or deep soil flipping (Schiedung et al., 2019) have also an important impact on the vertical distribution of C, but their sporadic application is more challenging to represent in models, particularly using equations for advection.

Vegetation change due to management alters the partitioning of primary production between above and belowground components and also the vertical distribution of root inputs and rhizodeposition (Rumpel & Kögel-Knabner, 2011). In models, changes in vegetation can have an influence on the total amount of carbon inputs entering the soil system, the shape of the decline of root inputs by depth, its partitioning between labile and stable fractions, and the production of DOC (Ota et al., 2013).

Exogenous C inputs such as biochar, compost, or biosolids to subsoil can be considered as C inputs differing in chemical and physical properties in comparison to regular C inputs from roots (Paustian et al., 2016). They alter the total amount and the vertical distribution of inputs to soils and can modify rates of microbial activity if the new inputs are highly degraded or strongly bound to mineral surfaces (Button et al., 2022; Rumpel et al., 2012).

3 | SOIL CARBON PROFILE MODELS

While the overwhelming majority of soil carbon models do not represent spatial processes (Manzoni & Porporato, 2009), a small number of models have been published that in some way account for the vertical soil carbon profile. For example, some models vertically distribute simulated total SOC or extrapolate topsoil carbon downwards using a predefined depth function, in order to determine lateral soil carbon transport due to erosion (Hilinski, 2001; Rosenbloom et al., 2001). Several models represent carbon pools in predefined soil layers that differ with respect to physical and chemical parameters, as well as temperature, moisture, and root input (Grant et al., 1993; van Veen & Paul, 1981). In some cases, heat or water transport between layers is included to account for the effects of temperature and moisture on decomposition or to simulate the leaching of mineral nitrogen (Hansen et al., 1991; Li et al., 1992). However, these models do not consider explicitly the vertical transfer of organic matter between layers. A number of models of DOC dynamics have been proposed (Brovelli et al., 2012; Gjettermann et al., 2008; Michalzik et al., 2003; Neff & Asner, 2001). These models account explicitly for the production and mineralization of DOC, as well as vertical transport with water flow and adsorption and desorption. Transport is usually represented as advection, based on measured or simulated water fluxes. These schemes are mainly developed to reproduce DOC fluxes and concentrations at small scales

and usually require site-level calibration or detailed information on soil texture.

The effects of bioturbation in terrestrial soils have been modeled in relation to the transport of radionuclides (e.g., Bunzl, 2002; Kaste et al., 2007; Müller-Lemans & van Dorp, 1996) and soil formation (Kirkby, 1977; Salvador-Blanes et al., 2007).

Perhaps the first model truly aimed at dynamically simulating the soil carbon profile was developed by Kirkby (1977) as part of a soil formation model. Since then, a number of models have been developed that combine decomposition with vertical transport, represented either as diffusion (Koven et al., 2009; O'Brien & Stout, 1978; van Dam et al., 1997), advection (Baisden et al., 2002; Bosatta & Ågren, 1996; Dörr & Münnich, 1989; Feng et al., 1999; Jenkinson & Coleman, 2008; Nakane & Shinozaki, 1978), or both (Braakhekke et al., 2011, 2013; Bruun et al., 2007; Elzein & Balesdent, 1995; Freier et al., 2010; Guenet et al., 2013; Koven et al., 2013). Most of these models were developed to explain measurements of carbon and tracer profiles. Increasingly, more models are now developed to represent soil carbon cycling and predict land–atmosphere carbon exchange (Ahrens et al., 2020; Huang et al., 2018; Koven et al., 2013; Luo et al., 2020; Tao et al., 2023; Tifafi et al., 2018; Wang et al., 2021) and the effect of land management practices on CS in soils (Jenkinson & Coleman, 2008; Keyvanshokouhi et al., 2019; Mary et al., 2020; Taghizadeh-Toosi et al., 2014).

3.1 | A general model of soil carbon transport and decomposition with depth

The main processes involved in the formation of soil carbon profiles—bioturbation, liquid phase transport, rhizodeposition, and decomposition—are commonly represented in models using the mathematical paradigms of diffusion, advection, and reaction, respectively. It is therefore useful to conceptualize models of soil organic matter (SOM) transport and dynamics by a general paradigm expressed as

$$\frac{\partial x(d,t)}{\partial t} = \text{Diffusion} + \text{Advection} + \text{Reaction}, \tag{1}$$

where the variable x represents SOM or carbon, and the variable t represents time. We use here partial derivatives (the ∂ symbol) to represent the change of soil carbon with respect to time, assuming that it can also change along a variable d that denotes soil depth. Therefore, we are also interested in representing changes in x with depth; that is, $\partial x / \partial d$. Equation (1) is a continuity equation, expressing how the conserved quantity x, which obeys mass conservation, changes continually with soil depth and time.

Our main postulate is that all models of vertical SOC transport are special cases of 1, expressing different forms of diffusion, advection, and reaction. This general approach to modeling vertical dynamics has been identified previously for diverse systems such as marine organic matter (Sarmiento & Gruber, 2006) or sediments (Arndt et al., 2013).

3.1.1 | Diffusion

Processes related to bioturbation and tillage are commonly represented in models using diffusion equations. A simple general model of soil carbon profile dynamics, including only vertical diffusion and inputs, can be expressed as

$$\frac{\partial x(d,t)}{\partial t} = \frac{\partial}{\partial d}\left(\kappa(d,t)\frac{\partial x(d,t)}{\partial d}\right) + u(d,t), \tag{2}$$

where $\kappa(d,t)$ is a function that represents how mass diffusivity depends on soil depth and time. Mass diffusivity is a soil property that generally does not change considerably over short timescales. Some models represent changes in diffusion with depth as a function of bulk density. In the most simple case, it can be expressed as a constant κ with no depth dependence. The function $u(d,t)$ expresses how litter and root inputs change with depth and time and can take multiple forms depending on attributes of the vegetation such as phenology, allocation, and rhizodeposition.

Models in the form of Equation (2) can only be solved (analytically or numerically) if initial conditions $x(d,0)$ are known, as well as the carbon contents or their change at two points along the vertical profile, between a depth at the surface d_0 and some maximum depth d_{max}. The latter are called the boundary conditions and must be known a priori in order to obtain solutions to these models.

To obtain an intuitive understanding of potential solutions to this model, it is useful to assume mass diffusivity as a constant (κ) and that inputs of organic matter to the soil are constant over time according to some function $u(d)$ where the inputs change with depth. Under these conditions, the soil carbon content along the profile reaches a steady state in which it does not change over time; that is,

$$\frac{\partial x(d,t)}{\partial t} = 0,$$

and the steady-state carbon content along the profile $x(d)$ is the solution to the second-order ordinary-differential equation

$$\frac{\partial^2 x}{\partial d^2} = -\frac{u(d)}{\kappa}. \tag{3}$$

Again, this equation can be solved using boundary conditions, integrating with respect to d to obtain the distribution of carbon content with depth $x(d)$. Equation (3) implies that the steady-state carbon content in a diffusion-controlled environment is mostly defined by the relation between the depth distribution of inputs and the mass diffusivity of the soil. The vertical distribution of inputs is mostly a property of the vegetation and the rhizosphere system, while mass diffusivity is mostly a property of the soil and the organisms that act as bio-engineers.

3.1.2 | Advection

The other main mathematical paradigm used to represent vertical processes in soil carbon profiles is advection, that is, the transport of organic carbon dissolved in water. Following mass conservation, advection can be expressed as

$$\frac{\partial x(d,t)}{\partial t} = -\frac{\partial}{\partial d} f(x(d,t)), \tag{4}$$

where $f(x(d,t))$ is the flux or flow rate of mass at depth d and time t. In other words, the mass of soil carbon can only change over time due to the flow rate of the fluid along a vertical direction. If the fluid is flowing at a constant velocity v, Equation (4) can be simplified to

$$\frac{\partial x(d,t)}{\partial t} = -v\frac{\partial x(d,t)}{\partial d}. \tag{5}$$

Intuitively, this implies that soil carbon is removed from a depth d at the velocity at which the fluid is passing through, and the gradient at which carbon content changes with depth. Flow velocity is determined by the combination of all the physical, chemical, and biological factors that affect water flow in saturated and unsaturated soils. Although flow velocity may not be constant in most cases, Equation (5) helps to understand its role in modeling SOM transport mechanisms in soils.

To better understand the role of $f(x(d,t))$ in Equation (4), it is useful to think of $x(d,t)$ as a density function (LeVeque, 1990) that represents the mass concentration of SOM at a particular depth and time. Therefore, the total mass of carbon between two depths d_1 and d_2 at time t is given by

$$\int_{d_1}^{d_2} x(d,t)\ \mathrm{d}d.$$

Because in an advection only system the total mass between the depths d_1 and d_2 only changes due to the flux at the end points, we can assume that

$$\frac{\mathrm{d}}{\mathrm{d}t}\int_{d_1}^{d_2} x(d,t)\mathrm{d}d = f\left(x\left(d_2,t\right)\right) - f\left(x\left(d_1,t\right)\right). \tag{6}$$

The function $x(d,t)$ is not known explicitly, therefore we do not have explicit formulas for the flow rates f. Nevertheless, Equation (6) helps to understand the role of the flow rate function f in Equation (4); it represents the flow rate of soil carbon at any given depth and time.

3.1.3 | Reaction (decomposition)

If we ignore vertical transport, soil carbon would display temporal dynamics related to the action of microorganisms and how they consume organic matter. This process of decomposition has been studied extensively, and there are hundreds of mathematical models that represent these dynamics ignoring vertical transport processes (Manzoni & Porporato, 2009). Despite the large variety of models, most of these models can be expressed in a general expression of the form (Sierra, Ceballos-Núñez, et al., 2018; Sierra & Müller, 2015)

$$\frac{\mathrm{d}\boldsymbol{x}}{\mathrm{d}t} = \boldsymbol{u}(\boldsymbol{x},t) + \mathbf{B}(\boldsymbol{x},t)\cdot\boldsymbol{x}(t). \tag{7}$$

This general model is expressed in vector (lower case bold) and matrix (upper case bold) form because it is assumed that SOC is highly heterogeneous, and different proportions decompose at different rates. Therefore, the vector $\boldsymbol{x}(t) \in \mathbb{R}^n$ represents the mass of soil carbon in n number of compartments at time t. The total mass at time t, $x(t)$, can be simply obtained as the sum of the elements of this vector, that is, $x(t) = \| \boldsymbol{x}(t) \|$ (the vertical bars represent a norm). Mass inputs to this system are represented by the vector $\boldsymbol{u}(\boldsymbol{x},t)$, which expresses the amount of organic matter inputs that would enter each compartment. Because above and belowground litter inputs can differ in their chemical and physical properties, different proportions of the total mass may enter different compartments. In addition, the inputs may depend on the amount of carbon in particular compartments; for example, if exudation rates depend on the amount of mycorrhiza. For this reason, the inputs $\boldsymbol{u}$ are expressed as dependent on the amount of mass present in the compartments at any given time.

Rates of decomposition and transfer of carbon among compartments are expressed in the matrix $\mathbf{B}(\boldsymbol{x},t)$ of Equation (7). This matrix is called compartmental because it has important mathematical properties related to mass conservation: all diagonal elements are non-positive, all off-diagonal elements are non-negative, and the column sums are non-positive (Metzler & Sierra, 2018; Sierra, Ceballos-Núñez, et al., 2018).

Linear models such as Century and RothC as well as nonlinear microbial models such as those proposed by soil ecologists (e.g., Allison et al., 2010; Schimel & Weintraub, 2003) are special cases of the general model of Equation (7) (Sierra & Müller, 2015), whose internal structure helps to study particular aspects of decomposition processes that are independent of vertical transport. These processes include differences in the decomposability of different types of organic matter, organo–mineral interactions, the effects of abiotic variables such as temperature, moisture, and pH on the rates of organic matter processing, and interactions between substrates and microbial groups, among others.

To incorporate vertical transport processes in this model, we can assume that at any given depth d, reaction (decomposition) processes are expressed as

$$\frac{\partial x(d,t)}{\partial t} = \left\| \frac{\mathrm{d}\boldsymbol{x}(d,t)}{\mathrm{d}t} \right\| \tag{8}$$

where the sum is over all the compartment contents at any given depth and time. Notice that this expression contains all the litter inputs entering the soil, split according to the compartments at which they enter.

3.1.4 | Combining transport and decomposition

In the previous sections, we analyzed the processes of diffusion, advection, and decomposition separately. Now we can combine them, following the general paradigm expressed in Equation (1). This general model has the form

$$\begin{aligned}\frac{\partial x(d,t)}{\partial t} &= \frac{\partial}{\partial d}\left(\kappa(d,t)\frac{\partial x(d,t)}{\partial d}\right) - \frac{\partial}{\partial d} f(x(d,t)) + \left\| \frac{\mathrm{d}\boldsymbol{x}(d,t)}{\mathrm{d}t} \right\|, \\ &= \frac{\partial}{\partial d}\left(\kappa(d,t)\frac{\partial x(d,t)}{\partial d}\right) - \frac{\partial}{\partial d} f(x(d,t)) + \|(\boldsymbol{u}(\boldsymbol{x},d,t) + \boldsymbol{B}(\boldsymbol{x},d,t)\cdot\boldsymbol{x}(d,t))\|. \end{aligned} \tag{9}$$

Most mathematical models of vertical carbon transport and decomposition should be special cases of this equation. It can lead to very complex dynamics resulting from the simultaneous effect of physical, chemical, and biological processes related to transport and decomposition.

Equation (9) cannot be solved analytically, but it can be discretized in time and space to obtain numerical solutions. The discretization approach consists of defining a fixed number k of depth intervals Δd where the solution of the partial differential equation is approximated using algebraic equations, and the system is then moved forward in time at discrete intervals Δt. Most numerical methods to approximate solutions to Equation (9) would attempt to find a vector $\boldsymbol{X} \in \mathbb{R}^{k+2}$ for k depth intervals by solving a linear equation of the form

$$\boldsymbol{A} \cdot \boldsymbol{X} = \boldsymbol{F}, \tag{10}$$

where the matrix $\boldsymbol{A}$ and the vector $\boldsymbol{F}$ result from the discretization of the original system using a finite-difference or a finite-element method (Lanczos, 1996; LeVeque, 2007). The dimension of this system is $(k+2)\times(k+2)$, with the two additional dimensions incorporating information based on the boundary conditions, which must be added to the discretized system and become an integral part of the new linear differential operator (Lanczos, 1996). Because after the discretization, mass conservation must be preserved, we postulate that the new system of equations must be compartmental. In other words, a discretized system representing the transport and decomposition of organic matter can be expressed as a compartmental system in the form of Equation (7). There are a few examples from the previous literature that may help to confirm this assertion. For instance, Metzler et al. (2020) showed that the soil carbon module of the ELM model (Koven et al., 2013), which contains 10 discrete depth layers and seven pools in each layer, can be approximated with a compartmental system that produces the exact same numerical solution as the original model that was developed with partial differential equations. Similarly, Huang et al. (2018) expressed the same model of Koven et al. (2013) as a system of linear equations in matrix form and found exact approximations to the original model.

The approximation of the nonlinear model expressed with partial differential equations is possible if the system is assumed at steady state. In the general model of Equation (9), the steady-state solution $x_{ss}(d)$ is obtained when $\partial x(d,t)/\partial t = 0$. At this steady state, the amount of carbon stored in the system does not change over time, and nonlinear interactions vanish. Therefore, the behavior of $x_{ss}(d)$ and a tracer such as ^{14}C, which is commonly used to parameterize SOC transport models, becomes linear with constant coefficients (Anderson, 2013). Thus, models of SOC dynamics with vertical transport can be expressed as linear systems with compartmental structure, assuming the system is at near steady state.

3.2 | The constant coefficient model and its steady-state solution

Despite the generality of the model of Equation (9) to represent vertical patterns of diffusion and advection, most of the models previously reported in the literature use constant diffusion and advection as well as constant decomposition and transformation rates (Table 1). Furthermore, most previous studies solve the model for the steady-state carbon content and analyze the resulting vertical patterns. Therefore, it is important to study in more detail a simplified version of the general model of Equation (9) for the case of constant coefficients at the steady state.

Assuming constant diffusion [$\kappa(d,t) = \kappa$ for all d and t] and constant flow velocity [$f(x(d,t)) = v\,x(d)$, with v constant for all d and t], we can write a steady-state version of Equation (9) by making the time derivative equal to zero as

$$\kappa\frac{\partial^2 x(d)}{\partial d^2} - v\frac{\partial x(d)}{\partial d} + g(d) = 0, \tag{11}$$

with $g(d)$ representing the balance between inputs and decomposition at each depth, also assuming constant decomposition and transformation rates at each depth [$\mathbf{B}(\boldsymbol{x},d,t) = \mathbf{B}(d)$ for all t], and a constant vector of inputs at each depth [$\boldsymbol{u}(\boldsymbol{x},d,t) = \boldsymbol{u}(d)$ for all t]. Therefore,

$$g(d) = \| \boldsymbol{u}(d) + \mathbf{B}(d)\cdot\boldsymbol{x}(d) \|. \tag{12}$$

Equation (11) is a general form of a linear second order differential equation with constant coefficients, for which a numerical solution can be obtained by discretizing the system along fixed depth intervals and solving the resulting system of linear equations as in Equation (10).

Two further simplified forms of the general equation can be found in the literature. The case in which advective transport is not considered relevant (e.g., O'Brien & Stout, 1978) and therefore

$$\kappa\frac{\partial^2 x(d)}{\partial d^2} + g(d) = 0, \tag{13}$$

or the case in which diffusive transport is not considered relevant (e.g., Baisden et al., 2002; Baisden & Parfitt, 2007; Feng et al., 1999)

$$-v\frac{\partial x(d)}{\partial d} + g(d) = 0. \tag{14}$$

TABLE 1 Summary of models representing C dynamics along the vertical profile using the diffusion–advection–reaction (DAR) paradigm.

Model/reference	Processes	d_{max} (m)	Ecosystem/location	n	v	κ	Péclet number
O'Brien and Stout (1978)	DR, Equation (13)	1.00	Managed pasture, NZ	1		$13.2\,cm^2\,year^{-1}$	0
Elzein and Balesdent (1995)	DAR, Equation (11)	1.65	Kattinkar, India	3	$0.13\,mm\,year^{-1}$	$5.15\,cm^2\,year^{-1}$	0.003
Elzein and Balesdent (1995)	DAR, Equation (11)	1.95	Pará, Brazil	3	$0.34\,mm\,year^{-1}$	$16.58\,cm^2\,year^{-1}$	0.002
Elzein and Balesdent (1995)	DAR, Equation (11)	1.63	Bahia, Brazil	3	$0.48\,mm\,year^{-1}$	$5.29\,cm^2\,year^{-1}$	0.009
Elzein and Balesdent (1995)	DAR, Equation (11)	0.52	Forest, Bezange, France	3	$0.6\,mm\,year^{-1}$	$0.94\,cm^2\,year^{-1}$	0.064
Elzein and Balesdent (1995)	DAR, Equation (11)	1.00	Forest, Marly, France	3	$0.42\,mm\,year^{-1}$	$1.48\,cm^2\,year^{-1}$	0.028
Feng et al. (1999)	AR, Equation (14)	1.00	Oak chaparral, USA	1	$1.51\,cm\,year^{-1}$		∞
Feng et al. (1999)	AR, Equation (14)	1.00	Pine, USA	1	$1.67\,cm\,year^{-1}$		∞
Feng et al. (1999)	AR, Equation (14)	1.00	Ceanothus chaparral, USA	1	$1.56\,cm\,year^{-1}$		∞
Feng et al. (1999)	AR, Equation (14)	1.00	Chamise chaparral, USA	1	$1.52\,cm\,year^{-1}$		∞
Baisden et al. (2002)[a]	AR, Equation (14)		<3 ky old grassland soil, USA	3	$[4.0, 0.47, 0.40]\,mm\,year^{-1}$		∞
Baisden et al. (2002)	AR, Equation (14)		200 ky old grassland soil, USA	3	$[4.0, 0.49, 0.39]\,mm\,year^{-1}$		∞
Baisden et al. (2002)	AR, Equation (14)		600 ky old grassland soil, USA	3	$[3.2, 0.28, 0.43]\,mm\,year^{-1}$		∞
Baisden et al. (2002)	AR, Equation (14)		3 My old grassland soil, USA	3	$[0.5, 0.26, 0.10]\,mm\,year^{-1}$		∞
Bruun et al. (2007)	DA, Equation (15)	0.55	Cropland, Denmark	0	$0.0081\,cm\,year^{-1}$	$0.71\,cm^2\,year^{-1}$	0.011
Baisden and Parfitt (2007)	AR, Equation (14)	1.00	15 ky old grassland soil, NZ	3	$[6.2, 0.9, 0.19]\,mm\,year^{-1}$		∞
Baisden and Parfitt (2007)	AR, Equation (14)	1.00	200 ky old grassland soil, NZ	3	$[0.6, 1.3, 0.25]\,mm\,year^{-1}$		∞
Baisden and Parfitt (2007)	AR, Equation (14)	1.00	600 ky old grassland soil, NZ	3	$[0.5, 0.5, 0.5]\,mm\,year^{-1}$		∞
Braakhekke et al. (2011)	DAR, Equation (11)	0.7	Deciduous forest, Germany	5	$0.002\,m\,year^{-1}$	$0.6\,cm^2\,year^{-1}$ [b]	0.333
Ota et al. (2013)	DAR, Equation (11)	1.5	Mediterranean grassland, USA	3			NA
Braakhekke et al. (2013)	DAR, Equation (11)	2.0	Pine forest, Netherlands	5	$0.0651\,m\,year^{-1}$	$0.0852\,cm^2\,year^{-1}$	76.402
Braakhekke et al. (2013)	DAR, Equation (11)	0.7	Deciduous forest, Germany	5	$0.00137\,m\,year^{-1}$	$0.6792\,cm^2\,year^{-1}$	0.202
Koven et al. (2013)	DR, Equation (13)	3.8	Global, non-permafrost	7		$1\,cm^2\,year^{-1}$	0
Ahrens et al. (2015)	DAR, Equation (11)	0.9	Coniferous forest, Germany	4	NA	$3.24\times10^{-10}\,m^2\,s^{-1}$	NA
Wang et al. (2021)	DR, Equation (13)	1.2	Global, non-permafrost	7		$8.55\times10^{-5}\,cm^2\,h^{-1}$	0

Note: Column on processes indicates the combination of diffusion (D), advection (A), and reaction/decomposition (R) included in the models together with the main equation that generalizes the model. Modified and updated from Koven et al. (2013).

[a]The model considers three separate values of v for each C pool.

[b]Assuming a bulk density of $1000\,kg\,cm^{-3}$.

To interpret data from pulse response experiments, some researchers have ignored the inputs and decomposition part of the model (e.g., Bruun et al., 2007) using an equation of the form

$$\kappa \frac{\partial^2 x(d)}{\partial d^2} - v \frac{\partial x(d)}{\partial d} = 0. \quad (15)$$

Models explicitly representing decomposition usually use one or three pools to represent decomposition as in most traditional models. More detailed representations of decomposition are presented in the model of Braakhekke et al. (2011, 2013), which represents five different pools, including a litter layer component clearly separating processes related to decomposition in the surface organic layer from processes more affected by vertical transport in the mineral horizons. Also, the model of Koven et al. (2013) used seven distinct C pools: coarse woody debris, three litter pools, and three mineral soil C pools.

In the COMISSION model, not only advective DOC transport is considered, but also advective transport of litter particles similarly as in sediment models (Ahrens et al., 2015, 2020). In the latest version of the model (Ahrens et al., 2020), advective litter transfer and particle diffusion are depth dependent. The model also considers nonlinear interactions among C pools, therefore it deviates from the constant linear coefficients model of Equation (11) and is in better analogy to Equation (9). Similarly, the models of Wang et al. (2021) and Tao et al. (2023) include nonlinear interactions among C pools, with the size of the microbial biomass pools interacting with the size of litter and mineral soil pools, but ignoring advection and treating diffusion as a constant across all depths.

Particularly interesting is the model of Elzein and Balesdent (1995), which follows the form of Equation (11) and includes advection, diffusion, and decomposition of three distinct pools. This model is rather useful because it includes a minimum of complexity to represent most relevant processes of a carbon transport model. It is also a useful model for parameterization against data on C and ^{14}C concentrations in vertical profiles.

Returning to our steady-state analysis of the constant coefficient model, we can solve the system for the first derivative and analyze individual components of this equation

$$\frac{\partial x(d)}{\partial d} = \frac{\kappa}{v} \frac{\partial^2 x(d)}{\partial d^2} + \frac{g(d)}{v}. \quad (16)$$

For the special case of one single pool with vertical root inputs represented by $u(d)$ and vertical decomposition rates by $k(d)$,

$$\frac{\partial x(d)}{\partial d} = \frac{\kappa}{v} \frac{\partial^2 x(d)}{\partial d^2} + \frac{u(d) - k(d)x(d)}{v}. \quad (17)$$

Equation (17) is very useful to analyze the shape of soil C profiles for cases in which the equilibrium assumption is reasonable. First, Equation (17) shows that the vertical change of C in a soil profile is inversely proportional to the advective movement of C, such as in the case of DOC transport. For large values of advection velocity (v), the rate of change of C by depth would be small, and the vertical C profile would resemble a vertical line. Second, the sign of the rate of change of C by depth is mostly determined by the difference between belowground C inputs and decomposition. At depths where the decomposition flux [$k(d)\ x(d)$] is larger than belowground inputs, the decrease of C by depth is maximum (maximum negative value). Third, the ratio between diffusion and advection velocity (κ / v), the inverse of the Péclet number (see below), influences how second-order transport processes affect the shape of the rate of change of the vertical C profile (Figure 1).

In the analysis of partial differential equations, the Péclet number, defined as the ratio of advection to diffusion, plays a very important role in determining the characteristics of the numerical solution, such as its numerical stability (LeVeque, 2007). In addition, the Péclet number can be used to determine the degree by which diffusion or advection may dominate the shape of a soil C profile (Figure 1).

If soil C always decreases with depth (Jobbágy & Jackson, 2000), the decomposition flux in Equation (17) must be dominant across the entire soil profile, so the rate of change with depth remains negative. In fact, this analysis suggests that the balance between lateral C inputs and decomposition is one of the main factors that affect the shape of soil C profiles, where a continuous decrease in soil C is commonly observed.

A corollary or implication provided by Equation (17) is that if the decrease in soil C with depth follows a simple exponential function, the right-hand side of Equation (17) must be a constant value for all depths. This situation seems unlikely given the different interacting process that occur in soil, and in fact, mathematical functions different than the simple exponential provide the best fit to observed data (Jobbágy & Jackson, 2000).

3.3 | Numerical example

We used Equation (17) to investigate the role of diffusion, advection, decomposition, and lateral inputs on the shape of idealized soil carbon profiles. We chose values of κ and v within the range of values obtained in previous models (Table 1) as well as representative functions for $k(d)$ and $u(d)$ within the range of previous studies (e.g., Elzein & Balesdent, 1995; Jackson et al., 1996, 1997; Koven et al., 2013).

To investigate the effect of diffusion and advection, we ran simulations with values of $\kappa = \{0.1,1,5,15\}\,cm^2\,year^{-1}$ and $v = \{0.1,1,5,10\}\,cm\,year^{-1}$ (Figure 2), with root inputs and decomposition following Equations (18) and (19) as described below. The results show that vertical transport processes tend to create a horizon with the largest rate of change in concentrations of C with depth (first derivative) close to the surface. This layer could be the result of either advection

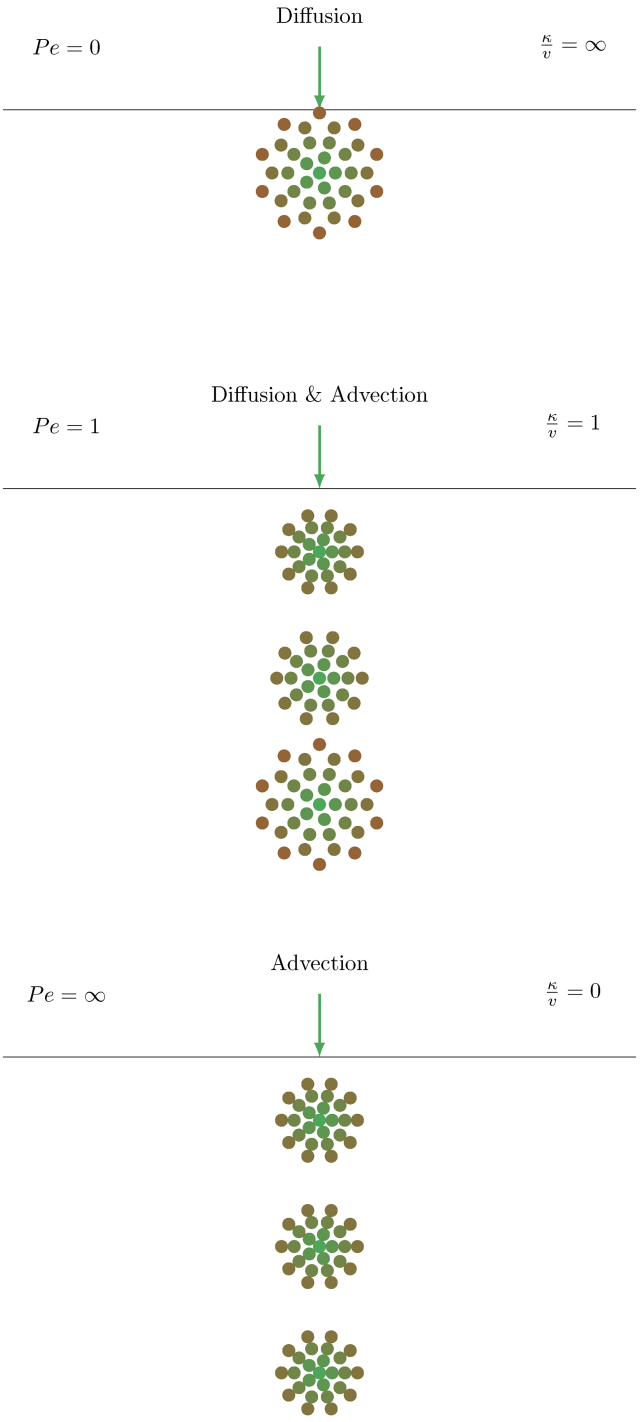

FIGURE 1 Schematic representation of the role of the Péclet number, which is the inverse of the ratio of diffusion to advection κ / v, on the type of vertical C transfer in a soil assuming a pulse of aboveground inputs. For a Péclet number of zero and $\kappa / v = \infty$, C entering the soil only moves due to diffusion (top); for a Péclet number and $\kappa / v = 1$, both diffusion and advection move the carbon vertically (center); for a Péclet number of ∞ and $\kappa / v = 0$, C is only moved vertically by advective processes as in the case of DOC transport (bottom).

or diffusion (Figure 2). Because in these simulations, lateral root inputs and decomposition decrease with depth (see Equations 18 and 19 below), there is a general trend of C concentrations to decline to values close to zero. Therefore, vertical transport do not seem to play a major role in transporting carbon below 50 cm depth within the range of advection and diffusion values used in these simulations, which covers the entire range of values obtained in previous studies (Table 1). Only at high advection velocities ($v = 10\,\text{cm year}^{-1}$) some carbon is transported below 50 cm depth, but this advection velocity is much higher than what has been used before in other models (Table 1).

The first derivative of the C concentration profiles with respect to depth from these simulations (Figure 2 right panels) showed negative derivatives for the entire depth profile. According to Equation (17), the first derivative can only be positive if lateral root inputs and transport processes dominate over the decomposition flux, which is not the case in these simulations. The decomposition flux dominates over all other processes, making the first derivative negative, although approaching zero at deeper layers. As advection velocity increased, the first derivatives were less negative, indicating that as advective transport increases the change in C concentrations by depth is less pronounced.

In a second set of simulations, we practically removed advection and diffusion by making the value of these coefficients very small ($\kappa = v = 0.01$) and represented lateral root inputs with the function

$$u(d) = -\beta^d \ln\beta. \tag{18}$$

This function predicts vertical root distributions and was originally proposed by Gale and Grigal (1987) and used by Jackson et al. (1996, 1997) to obtain vertical root distributions at the biome level. The original function predicts the fraction of root biomass for each depth, and multiplied by an average root turnover rate of $1\,\text{year}^{-1}$ (Gill & Jackson, 2000), it gives the proportion of root inputs per depth interval $u(d)$. For the simulations, we used values of β: {0.92,0.95,0.98} that include the observed extremes of values for shallow root systems ($\beta = 0.92$) and deep root systems ($\beta = 0.98$) (Gale & Grigal, 1987; Jackson et al., 1996).

The function used to represent decomposition rates by depth was extracted from Koven et al. (2013).

$$k(d) = k_0 \exp\left(\frac{-d}{d_e}\right), \tag{19}$$

with the maximum decomposition rate at the surface given by $k_0 = k(d = 0)$, and d_e representing the e-folding depth of decomposition rates. In our simulations, we used values of k_0: {1,0.1,0.01}year^{-1} and a constant value of $d_e = 90\,\text{cm}$. Equation (19) is an empirical function that accounts for unresolved processes such as changes in oxygen availability or microbial activity with depth, and therefore it could be considered as a place holder for other mechanistic representations of depth-dependent microbial dynamics.

The results from this second set of simulations evaluating the effect of lateral root inputs and decomposition showed that slowing down decomposition can have a significant effect on the shape of the vertical soil C profile (Figure 3). These results seem counterintuitive because Equation (17) suggests that the negative term of the

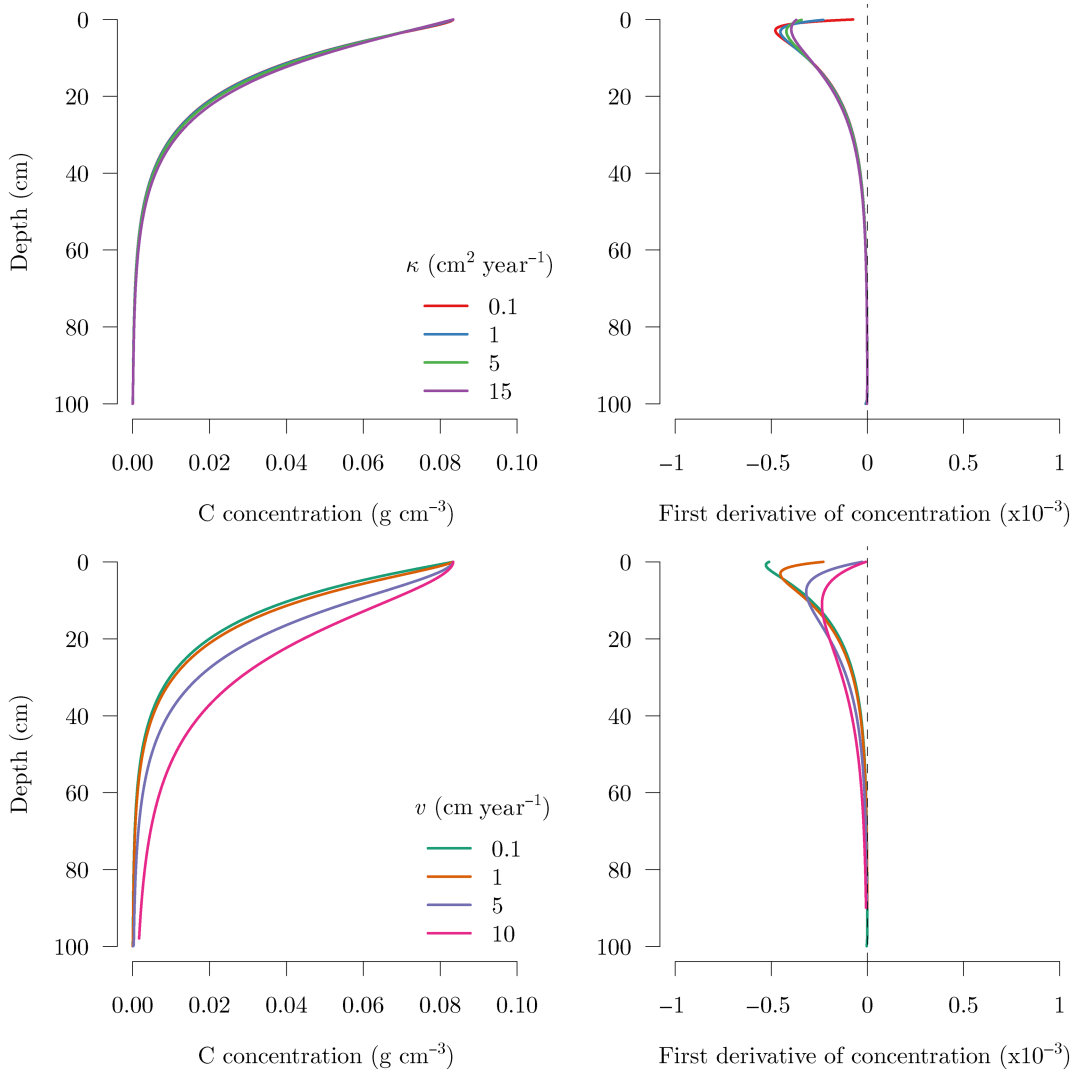

FIGURE 2 Numerical simulations of soil C depth profiles using the linear model with constant coefficients of Equation (17). The top panels show the C concentration and the first derivative of C concentrations for different values of the diffusion coefficient κ and a fixed value of advection velocity $v = 1\,\text{cm year}^{-1}$. The bottom panels show C concentrations and their first derivative for different values of v and a constant value of $\kappa = 1\,\text{cm}^2\,\text{year}^{-1}$.

equation should be affected by larger values of $k(d)$, but because with slow decomposition, higher amounts of C are obtained at steady state, the entire term $k(d)x(d)$ is large, promoting a strong soil C gradient. The vertical distribution of root inputs also has a significant effect on the shape of the soil C profile, with shallow root inputs promoting a strong vertical gradient and deep-rooting systems a more pronounced gradient with lower values of the first derivative (Figure 3). In this set of simulations, we also observed a maximum rate of change of C at the upper layers, where the value of the first derivative reached a maximum.

Parameter values for diffusion, advection, root input distribution, and decomposition rates with depth are highly uncertainty, and there is little information on their global distribution across biomes. To test uncertainty in the components of Equation (17), we performed an uncertainty analysis following a Monte Carlo uncertainty approach. We chose 1000 random variates of the parameters κ and v from a uniform distribution within the range of observed values in Table 1, and ran simulations to obtain an estimate of prediction uncertainty in C concentration across depth (Figure 4). These simulations clearly show that uncertainty due to the diffusion parameter κ is much smaller than prediction uncertainty due to parameter v (Figure 4b). Similarly, we ran simulations with 1000 random variates of parameters β and d_e to test the effect of uncertainty in root inputs and decomposition rates, respectively. The results showed that prediction uncertainty is larger due to the depth distribution of decomposition than to the depth distribution of root inputs (Figure 4d), and both process dominate prediction uncertainty in comparison to uncertainty in transport processes (κ and v uncertainty).

Overall, the sensitivity analysis presented in Figures 2 and 3 and the uncertainty analysis in Figure 4 indicate that the vertical distribution of root inputs and decomposition play a larger role in

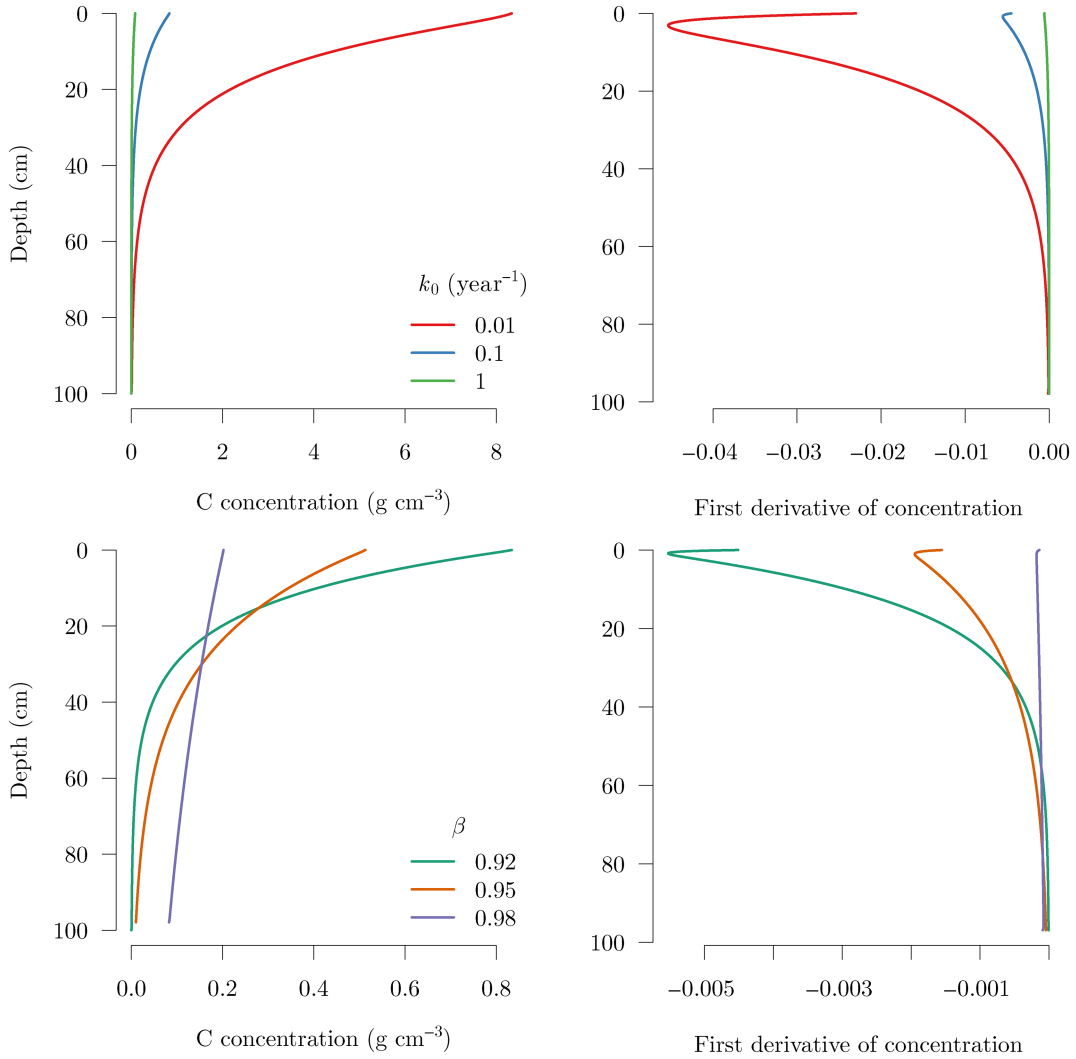

FIGURE 3 Numerical simulations of soil C depth profiles using the linear model with constant coefficients of Equation (17). The top panels show C concentration and its first derivative with respect to depth for different functions representing decomposition rate $k(d)$ (Equation 19). The different lines are the result of the model for different values of the maximum decomposition rate at the surface k_0, with the value of $k_0 = 1\,\text{year}^{-1}$ representing fast decomposition and $k_0 = 0.01\,\text{year}^{-1}$ slow decomposition. The lower panels represent the results of simulation for different shapes of the root input profile according to Equation (18), with the parameter $\beta = 0.98$ representing deep root inputs and $\beta = 0.92$ shallow root inputs.

determining the shape of soil carbon profiles than transport processes represented as diffusion and advection.

4 | ASSESSING C SEQUESTRATION AND THE FATE OF NEW C INPUTS

4.1 | Fate, transit time, and CS in the subsoil

In the context of climate change mitigation, we are generally interested in evaluating the capacity of soils for storing carbon at relevant timescales associated with management and policy outcomes. In many cases, we are interested in comparing different soils, and in other cases, we are interested in evaluating the effectiveness of different soil management practices. In any case, we need to use appropriate metrics to evaluate the environmental benefit of CS.

If we aim at promoting soil C sequestration, it is then important to analyze the fate of new inputs entering the soil, assess for how long the new carbon remains stored, and how much warming can be avoided while the C is stored (Crow & Sierra, 2022; Sierra, Crow, et al., 2021). For this purpose, we can use the following metrics: fate, transit time, and CS, which are mathematically defined as follows.

For a compartmental system in equilibrium, where carbon inputs are balanced with C losses, the fate of C entering at a time t_0 can be obtained as a function that predicts the mass of C remaining in the soil at time t; thus, we define $\tau = t - t_0$ and

$$\boldsymbol{m}(\tau) = e^{\tau \mathbf{B}}\ \boldsymbol{u}, \tag{20}$$

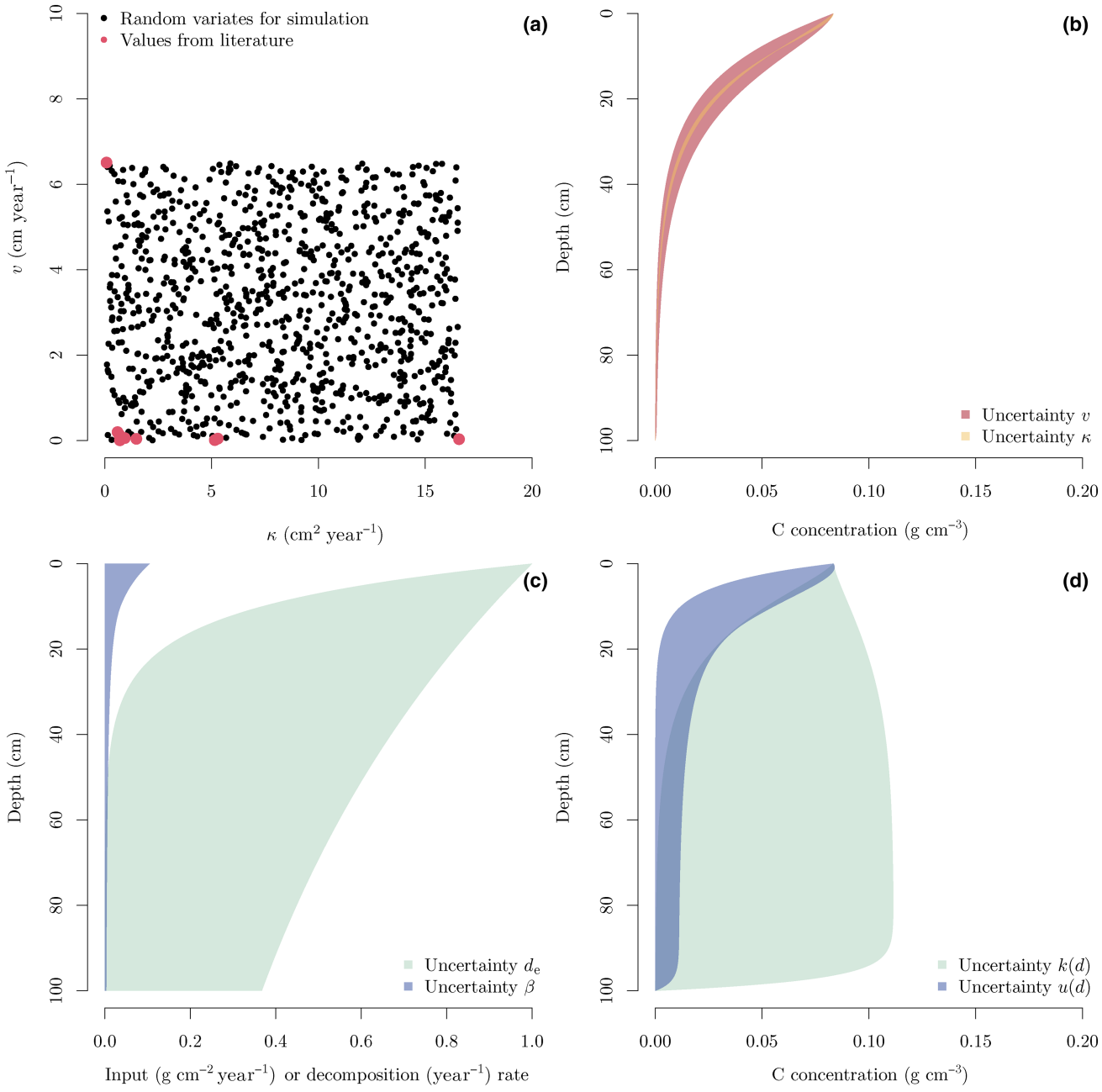

FIGURE 4 Uncertainty analysis based on the components of Equation (17) using a Monte Carlo uncertainty approach in which 1000 random variates of model parameters were chosen from a uniform distribution *U*. (a) Set of 1000 random variates of the diffusion coefficient $\kappa \sim U(0.09,16.58)$ and the advection velocity $v \sim U(0.01,6.51)$, and the set of values available from the literature (Table 1). (b) Prediction uncertainty in carbon concentration due to uncertainty in diffusion coefficient κ and advection velocity *v*. (c) Uncertainty in the distribution of root inputs [$u(d)$] due to uncertainty in parameter $\beta \sim U(0.9,1.0)$, and uncertainty in decomposition rate distribution [$k(d)$] due to uncertainty in parameter $d_e \sim U(10,100)$. (d) Prediction uncertainty in carbon concentration due to uncertainty in root input distribution [$u(d)$] and decomposition rate distribution [$k(d)$].

as in Sierra, Estupinan-Suarez, and Chanca (2021), where $\boldsymbol{m}(\tau)$ is a vector with the mass remaining for each compartment. This mass remaining is related to the transit time of carbon, which is defined as the time it takes carbon atoms to pass through the entire network of compartments until C leaves the soil system (Bolin & Rodhe, 1973; Manzoni et al., 2009; Sierra, Ceballos-Núñez, et al., 2018). The transit time distribution of carbon can be expressed as (Metzler & Sierra, 2018)

$$f_T(\tau) = -\mathbf{1}^\top \mathbf{B}\, e^{\tau \mathbf{B}} \frac{\boldsymbol{u}}{\| \boldsymbol{u} \|}, \tag{21}$$

and represents the relative proportion of carbon leaving the system at a time τ. In soils, transit time distributions generally have a long tail, indicating that most carbon entering soils are respired quickly, but small proportions can stay for long times (Sierra, Hoyt, et al., 2018).

Carbon sequestration is the storage of a certain amount of carbon over a certain period of time. It evaluates the fate of new inputs entering the soil integrated over a time horizon. The amount of sequestration quantified by the CS metric depends on both the amount of input entering the soil and the time it takes for this carbon to return to the atmosphere in the form of respiration. This amount of time is proportional to the transit time of carbon.

For a compartmental system at equilibrium, CS can be obtained as (Sierra, Crow, et al., 2021)

$$\mathrm{CS}(t) = \int_{t_0}^{t} \| \, \mathrm{e}^{\tau \, \mathbf{B}} \, \boldsymbol{u} \, \| \, \mathrm{d}\tau, \tag{22}$$

which is the integral of the total amount of mass remaining in the soil from a cohort of inputs entering at t_0.

If a particular transport-decomposition model can be discretized and expressed as a compartmental system following standard numerical methods (Lanczos, 1996; LeVeque, 2007), one can use Equations (20)–(22) to quantify the fate, transit time, and CS of a particular soil and compare results with those from another soil or with the outcomes of different forms of management.

Alternatively, $\boldsymbol{m}(t)$ and $f_T(\tau)$ can be obtained using impulse response experiments with existing transport models that are difficult to express as a compartmental system (Metzler & Sierra, 2018; Thompson & Randerson, 1999). The approach consists of running a model until reaching equilibrium, and at this point add a pulse of carbon and observe the mass remaining of the pulse over time, which is an approximation to $\boldsymbol{m}(t)$. One can also observe the respiration flux after the addition of the pulse, which is an approximation to the transit time distribution $f_T(\tau)$ (Metzler & Sierra, 2018). The results from pulse response experiments should provide very valuable information to assess the fate of new inputs entering the soil and whether they remain for relevant periods of time.

4.2 | Numerical example

In the previous example, we saw that transport, decomposition, and lateral root inputs play an important role in determining the shape of soil C profiles at equilibrium. We evaluate now with an example how fast/slow transport, combined with fast/slow decomposition in soil profiles, can affect the fate, transit time, and CS of a soil. Our aim is to assess the fate of new carbon inputs and whether they remain in soil for timescales relevant for climate change mitigation.

Given that our previous example showed that diffusion plays a minor role in comparison to advection for moving carbon downwards, we set a fixed value of $\kappa = 1\,\mathrm{cm^2\,year^{-1}}$ and varied the values of v. For simulations with fast transport, the values were $v = 5\,\mathrm{cm\,year^{-1}}$, and for simulations with slow transport $v = 0.1\,\mathrm{cm\,year^{-1}}$. Decomposition rates were considered fast with values of $k_0 = 1\,\mathrm{year^{-1}}$ and slow with $k_0 = 0.1\,\mathrm{year^{-1}}$ at the surface (Table 2) and declining with depth according to Equation (19). In all simulations, we considered a root input profile with an intermediate value of $\beta = 0.95$, that is, not too shallow nor too deep roots.

Simulation results showed that most C inputs entering at any given time only stay in the soil a few years, and only under slow decomposition, some C may remain for a few decades (Figure 5; Table 2). Decomposition rates seem to play a stronger control on the fate of C inputs than vertical transport rates. Under fast decomposition, most carbon was lost in 5 years independently from transport velocity, and very small proportions traveled through the soil profile because the carbon was decomposed before it had a chance to move downwards. Under slow decomposition and fast transport, some carbon is preserved longer because it decomposes at slower rates at deeper layers, but eventually this transported carbon is also decomposed in a few decades (Figure 5).

The transit time distribution of C through the entire soil profile for these different simulations showed that the large majority

TABLE 2 Parameters used and results obtained for simulations evaluating the effect of transport and decomposition on the fate, transit time, and CS of new inputs.

	Tf–Df	Tf–Ds	Ts–Df	Ts–Ds
κ ($\mathrm{cm^2\,year^{-1}}$)	1.000	1.000	1.000	1.000
v ($\mathrm{cm\,year^{-1}}$)	5.000	5.000	0.100	0.100
k_0 ($\mathrm{year^{-1}}$)	1.000	0.100	1.000	0.100
β	0.950	0.950	0.950	0.950
Proportion remaining after 1 year	0.449	0.914	0.424	0.875
Proportion remaining after 10 years	0.002	0.480	0.001	0.392
Proportion remaining after 50 years	0.000	0.000	0.000	0.022
Mean transit time (years)	1.333	9.699	1.217	11.498
Median transit time (years)	0.859	9.444	0.799	7.096
CS ($t \to \infty$)	16.028	363.721	12.587	133.416

Abbreviations: CS, carbon sequestration; Tf–Df, transport fast, decomposition fast; Tf–Ds, transport fast, decomposition slow; Ts–Df, transport slow, decomposition fast; Ts–Ds, transport slow, decomposition slow.

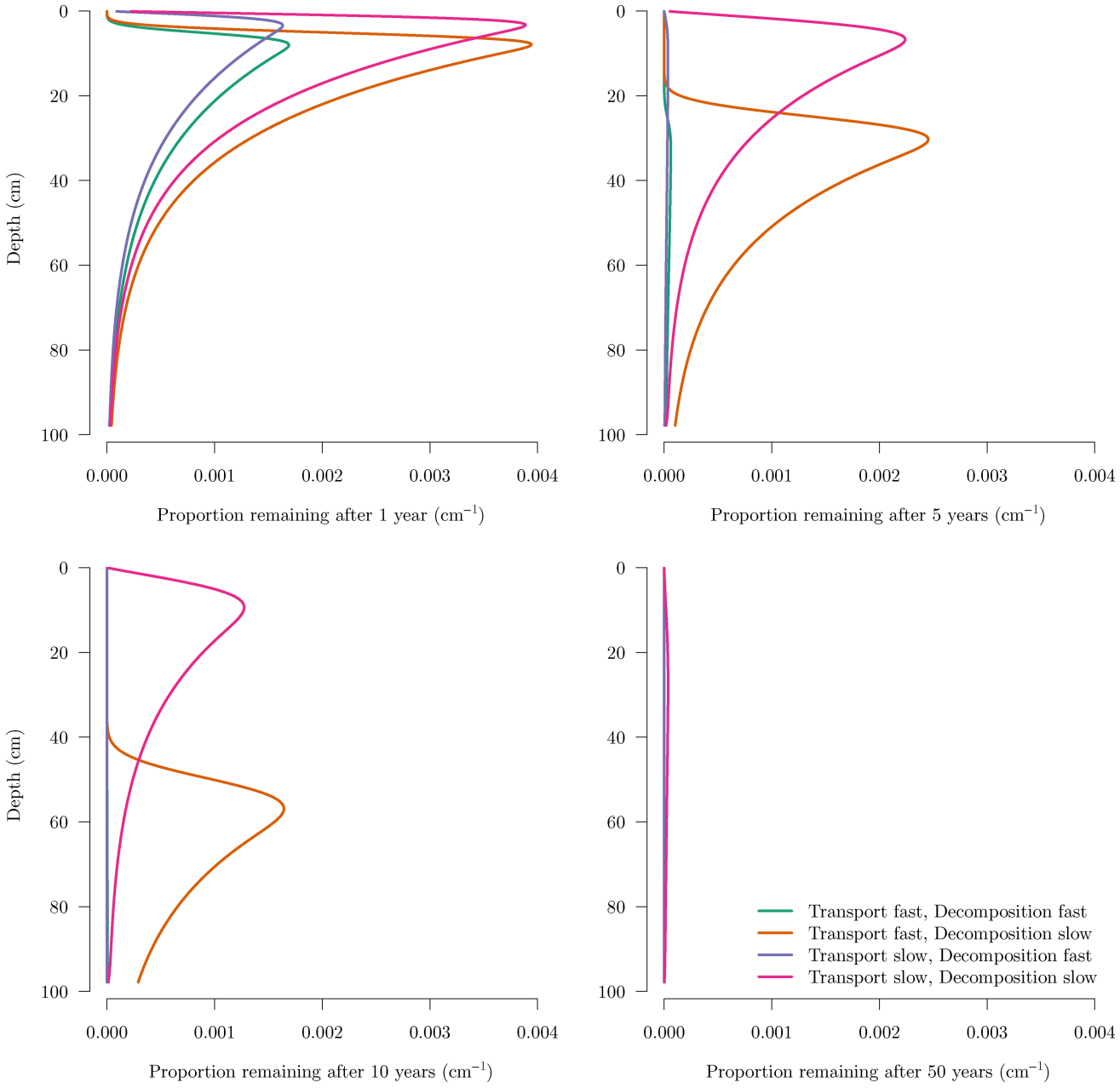

FIGURE 5 Proportion of C remaining in a soil profile of an amount of lateral inputs entering the soil at $t = 0$ represented by Equation (18) with $\beta = 0.95$. After 50 years, most of the carbon that entered at $t = 0$ is not present in the soil, even for the scenario with slow transport and decomposition rates.

of C entering the soil at any given time is lost within the first year (Figure 6a). Fifty percent of the C that enters the soil is lost in 0.86 years in the scenario with fast decomposition and fast transport, while in the scenario with slow decomposition and fast transport, 50% of the new carbon is lost in 9.4 years (Table 2). The slow decomposition scenarios showed a very different tail in the transit time distribution compared to the fast decomposition scenarios, with a larger proportion of carbon staying for longer times under slow decomposition. Therefore, the mean transit time is influenced by these long tails, with a mean transit time of 1.3 years in the fast transport slow decomposition scenario, and 11.5 years in the slow transport slow decomposition scenario (Table 2a). Despite slow decomposition, however, most of the new inputs do not stay for timescales beyond a few decades at the maximum.

At steady state, significantly more carbon is stored in the case of slow decomposition, particularly in the scenario of fast transport and slow decomposition (Figure 6b). However, to reach these large steady-state C concentrations, very long timescales of carbon accumulation are required. According to the transit time distributions, very small amounts of new C inputs remain in the long term; therefore, it would take a considerably long time (beyond decades) to reach these steady-state C values.

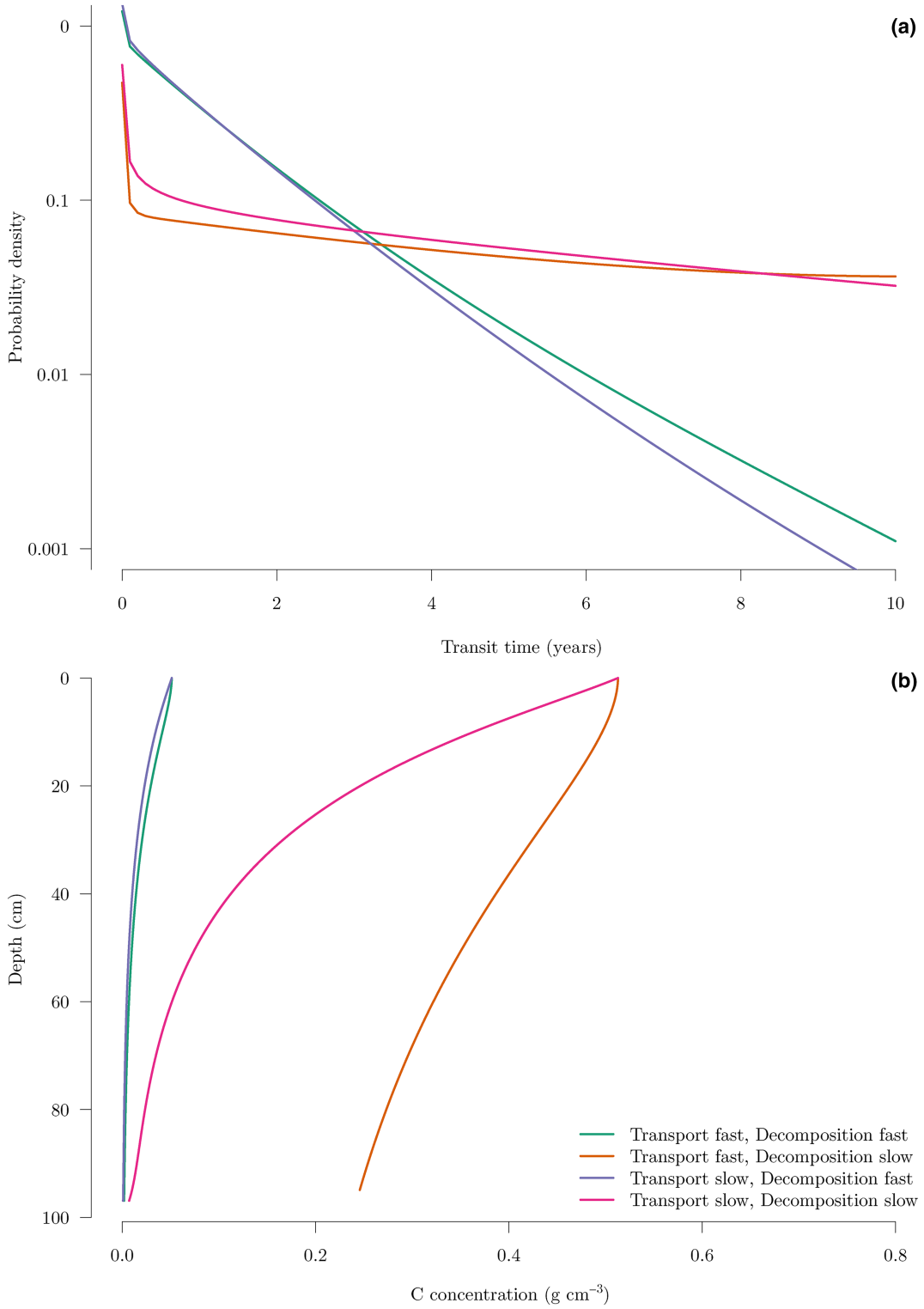

FIGURE 6 (a) Transit time distributions for four different scenarios of transport and decomposition in the subsoil. These distributions represent the proportion of C leaving the soil system at different times since C entered the soil. Note the logarithmic *y* axis. (b) Values of C concentration along the depth profile at steady state.

5 | EMPIRICAL EVIDENCE FROM SOIL PROFILES

The two numerical examples from the previous section suggest that (i) the change of soil C with depth is largely influenced by the difference between root inputs and decomposition and, to a lesser degree, by vertical transport processes such as diffusion and advection; and (ii) most new carbon inputs entering the soil do not remain stored for long timescales. In the following section, we will explore global-scale datasets of soil C profiles to test whether

these theoretical model predictions have empirical support based on observations.

5.1 | The shape of the vertical C profile across regions

The International Soil Radiocarbon Database (ISRaD) is a comprehensive and well-curated collection of soil carbon and radiocarbon data (Lawrence et al., 2020). We used version 1.7.8 of the database and extracted information on soil C concentration with depth down to 1 m. Data from 600 individual profiles were grouped by Köppen-Geiger climate zones (Beck et al., 2018) and averaged by 1 cm depth increments. Volcanic soils (classified as such in the field) were treated as a separate group given their distinct vertical C profile. A mass-preserving spline function (equal-area quadratic smoothing spline) was applied to each profile to account for the varying depth intervals in which samples across profiles were taken (Bishop et al., 1999; Ponce-Hernandez et al., 1986). This spline function interpolates C concentration for a continuum of depths, that is, an approximation to the function $x(d)$ for each of the groups (Figure 7).

Soil carbon decreased rapidly with depth in most soil profiles, reaching values close to zero at 1 m depth (Figure 7), with the

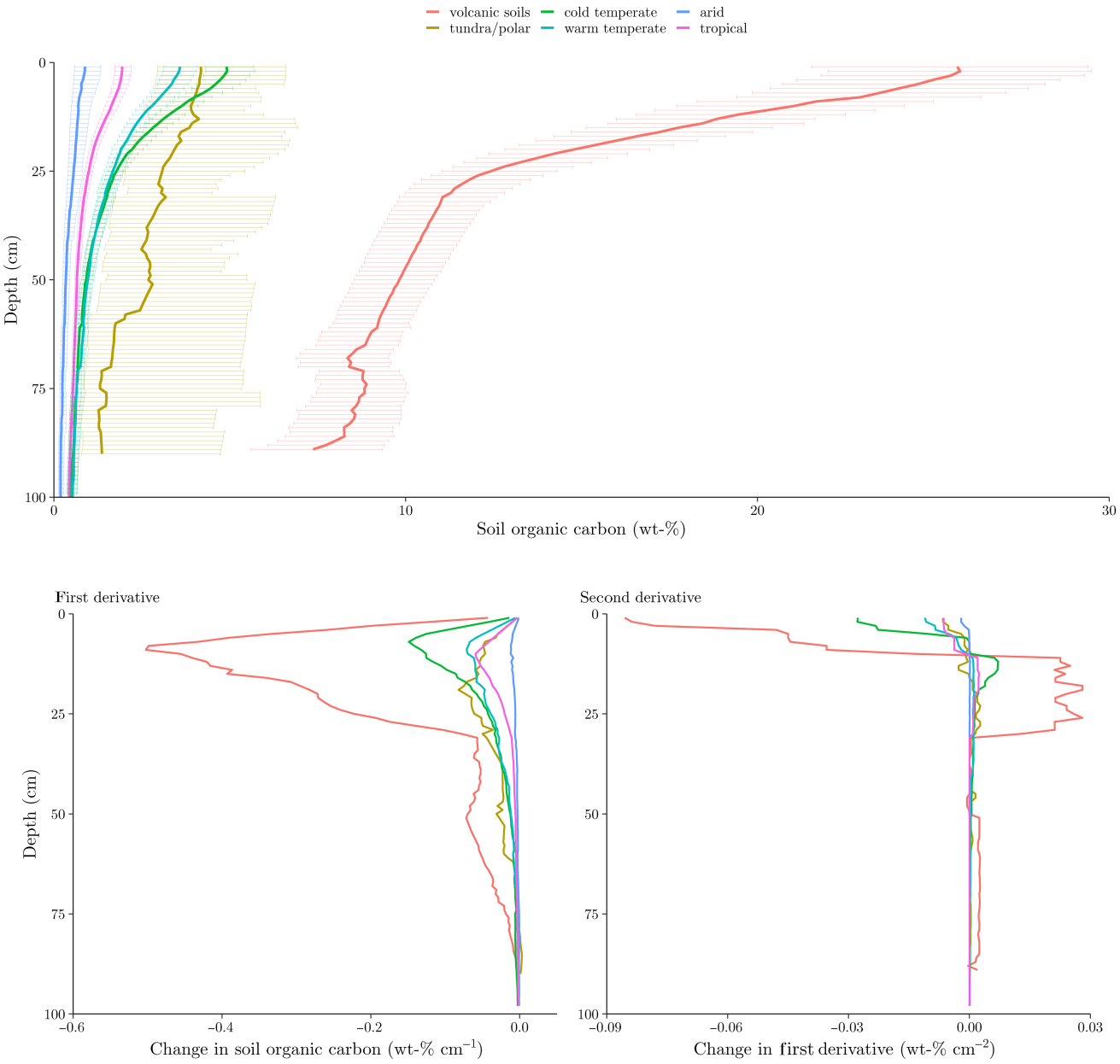

FIGURE 7 Soil carbon concentrations with first and second derivatives with respect to depth obtained from the International Soil Radiocarbon Database, with data from 600 profiles aggregated by biogeographical regions. Thick lines for each group represent the mean across available observations and are fitted to a spline curve. Horizontal lines represent the standard deviation across available observations.

exception of soils from tundra/polar regions and volcanic soils, which still contain relatively large quantities of C at 90 cm depth. Please note that these values are reported as concentrations with respect to the mass of soil. Bulk density data is not commonly reported for individual profiles and much less for individual depth horizons. Therefore, comparisons with the simulation experiments from previous sections must be done only with respect to qualitative aspects and not with respect to quantitative values.

The first derivative of soil C concentrations with respect to depth [$\partial x(d) / \partial d$, Figure 7] was negative for all groups, indicating that soil C always decreases with depth for these aggregated profiles. This is in agreement with our previous simulations, in which the first derivatives were always negative. We observed for all groups a peak in the first derivative where it reaches a maximum negative value, indicating that soil C decreases more strongly at some intermediate depth between 10 and 20 cm (Figure 7). According to Equation (17), a maximum negative value of the first derivative can only occur at depths where the microbial decomposition flux [$k(d)x(d)$] has its maximum value, that is, when microbes are consuming the maximum amount of carbon possible.

The value of the first derivative had the largest values overall for volcanic soils and the lowest values for arid soils. In both cases, decomposition rates may be slow compared to other soils; in volcanic soils, the presence of amorphous non-crystalline surfaces promote the sorption of organic matter into minerals and therefore slow decomposition and strong C accumulation (Crow et al., 2015; Marin-Spiotta et al., 2011); in arid soils low moisture availability leads to slow decomposition rates, but also low primary productivity, which leads to low carbon stocks (Moyano et al., 2013; Sierra et al., 2015). Therefore, the negative values of the first derivative are strongly dependent on the C stocks [$x(d)$] and, to a lesser extent, on the decomposition rate [$k(d)$]. The decomposition rate obviously plays a major role in determining the size of the C stock in conjunction with the input fluxes at depth, but the rate of decline of C with depth is mostly influenced by the resulting C stock. In addition, the last term of Equation (17) also reveals that for systems with slow advection velocities v approaching zero, small differences between lateral inputs and decomposition may be amplified. In other words, the large values of the negative derivative for the volcanic soils may be the result of very low advective movement of DOC, amplifying small differences between lateral inputs and decomposition.

Overall, the data from soil C profiles aggregated by regional groups and volcanic soils provide evidence supporting the idea that vertical transport may play a secondary role in determining the rate of soil C decrease with depth. The difference between lateral root inputs and decomposition may play a primary role in determining the shape of soil C profiles, and this difference may be amplified at low advection velocity rates. Diffusive movement of soil C seems to play a small role in these aggregated groups, something suggested by the low values of the second derivative (Figure 7); however, diffusion may have some control on the peak of C decrease found close to the surface in these profiles.

5.2 | Transit times of C from vertical profiles

Using data from ISRaD and a dataset on root input profiles, Xiao et al. (2022) obtained estimates of mean ages and mean transit times for soil C profiles at the global scale. The global averages revealed that the mean transit times of C are always younger than the mean age of C stored at all soil depths (Figure 8). In other words, despite the C stored in the soil being hundreds to thousands of years old, the C respired is only a few years to decades old. This result is consistent with our transit time simulations, which showed mean transit times of only a few years (Figure 6; Table 2). However, the actual values of mean transit time obtained from the data are actually much higher than those from the model results. This is to be expected given that the model used for the example only considered one single pool with a relatively fast decomposition rate, but in reality, soil carbon is highly heterogeneous and a significant proportion of its total carbon cycles at much slower rates, which would contribute to longer transit times. In addition, sorption of organic matter to mineral surfaces may increase with depth, making the overall decomposition of C at depth more limited (Ahrens et al., 2020). Nevertheless, model simulations and observations agree in that new C inputs to soil only remain stored in timescales of years to decades.

Fast mean transit times were observed for tropical forest, grassland, and cropland soils, while long transit times in the order of decades to centuries were only observed for tundra and boreal forest soils (Figure 8). These results are consistent with the idea that low temperatures and energy limitation may play a significant role in controlling the transit time of C at the biome level (Lu et al., 2018; Sierra et al., 2023; Xiao et al., 2022), with fast transit times in warm regions and longer transit times in cold high-latitude regions.

Because transit times are directly related to CS (Equations 21 and 22), we expect only tundra and boreal forest soils to store C in the subsoil at timescales relevant for climate change mitigation, that is, in the order of decades to centuries. In fact, previous studies have found that a large proportion of carbon used by microorganisms in the subsoil is recent and does not contribute to C stabilization in the subsoil (Balesdent et al., 2018; Scheibe et al., 2023). Therefore, we would expect lower values of CS for tropical forests, grasslands, and cropland soils in comparison with boreal forests and tundra soils. However, it is important to keep in mind that productivity in these high-latitude regions is relatively low compared to temperate and equatorial latitudes (Xiao et al., 2023). CS, as defined in Equation (22), accounts for this trade-off between the amount of inputs and its transit time through the soil, and it can be used to more specifically assess the climate mitigation potential of specific amounts of C added to the soil.

6 | IMPLICATIONS FOR SOIL C MANAGEMENT

Our analysis of a general model of soil C profile formation, together with the analysis of observations of soil carbon concentrations and

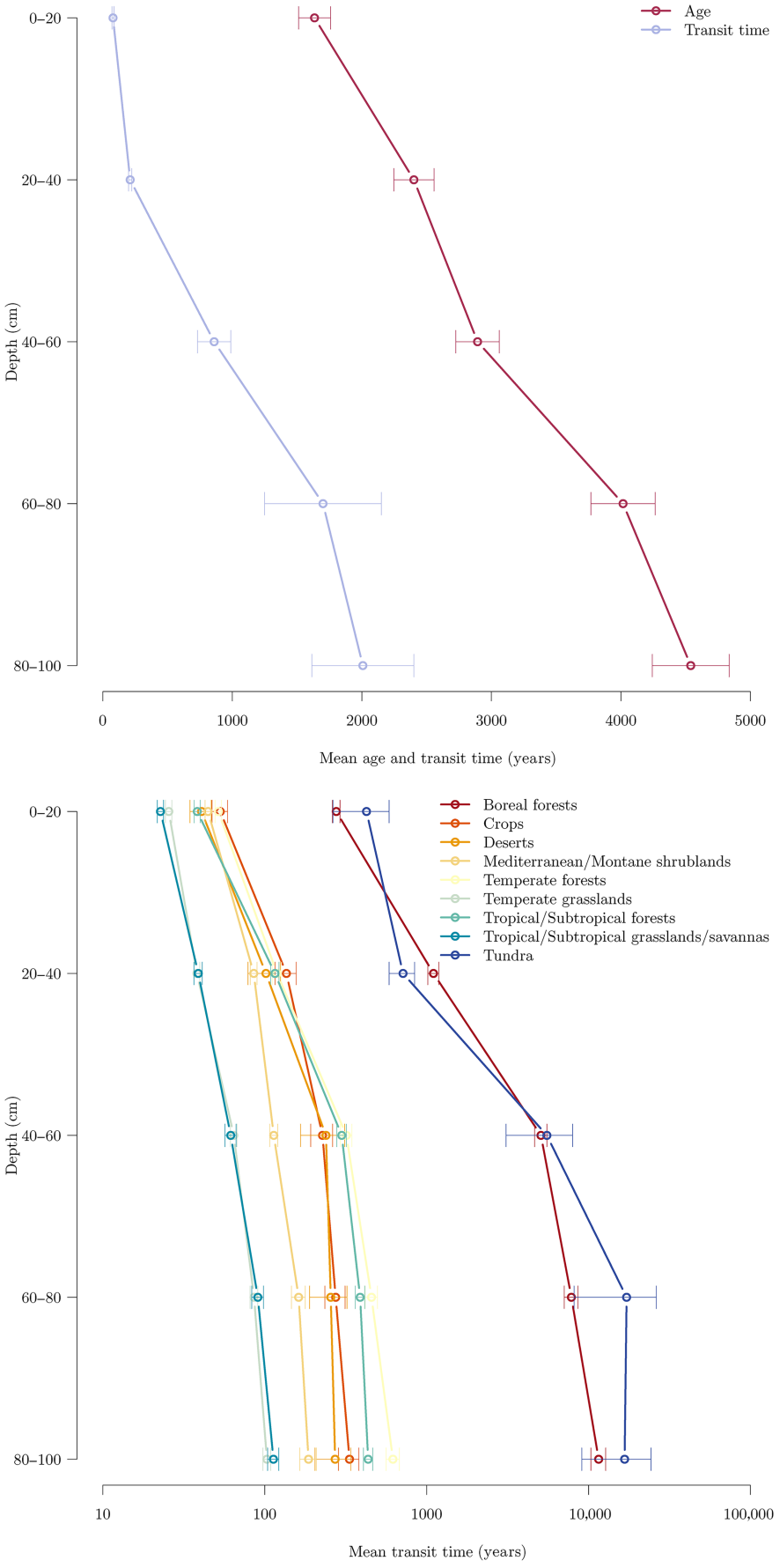

FIGURE 8 Estimates of mean age and mean transit time of carbon based on measurements of root inputs and soil radiocarbon obtained from ISRaD. The upper panel shows global-scale average values of mean age and mean transit time. The lower panel shows averages of mean transit time aggregated by biome.

transit times, provide relevant insights that can inform land management for CS and climate change mitigation. Even though current observations show that C concentrations decrease strongly with depth in most soils and new C inputs transit relatively fast, there are potentials to increase C storage with depth and increase the transit time of carbon across the entire profile.

If soils would be managed to increase subsoil C storage, the change of C concentrations with depth should be less dramatic and change less with respect to topsoil (Figure 9). From Equation (16), it can be inferred that a management objective could be framed in terms of keeping the first derivative of C concentration with respect to depth close to zero, so the storage of carbon in subsoil remains relatively similar to levels in topsoil. Using the model of constant advection and diffusion coefficients at steady state (Equation 16), we can frame this management objective as

$$\frac{\partial x(d)}{\partial d} = \frac{\kappa}{v}\frac{\partial^2 x(d)}{\partial^2 d} + \frac{g(d)}{v} = 0, \tag{23}$$

and because the derivative of a constant value of zero is equal to zero, the second derivative term vanishes from this equation, and the management objective reduces to

$$\frac{g(d)}{v} = 0. \tag{24}$$

This equation suggests that an effective way to achieve the goal of increasing C storage in the subsoil would be through increasing advective transport of C from top to subsoil, that is, increasing values of v so the ratio of Equation (24) approaches zero (Figure 9). Provided C inputs are high, their vertical advective movement should contribute to increase total carbon storage. In other words, even though vertical C transfer does not seem to play a significant role in explaining current data on soil C profiles, management activities could be implemented to increase vertical C transfers to horizons where it can be stabilized on available mineral surfaces (cf. Ahrens et al., 2020; Georgiou et al., 2022) and protect it from

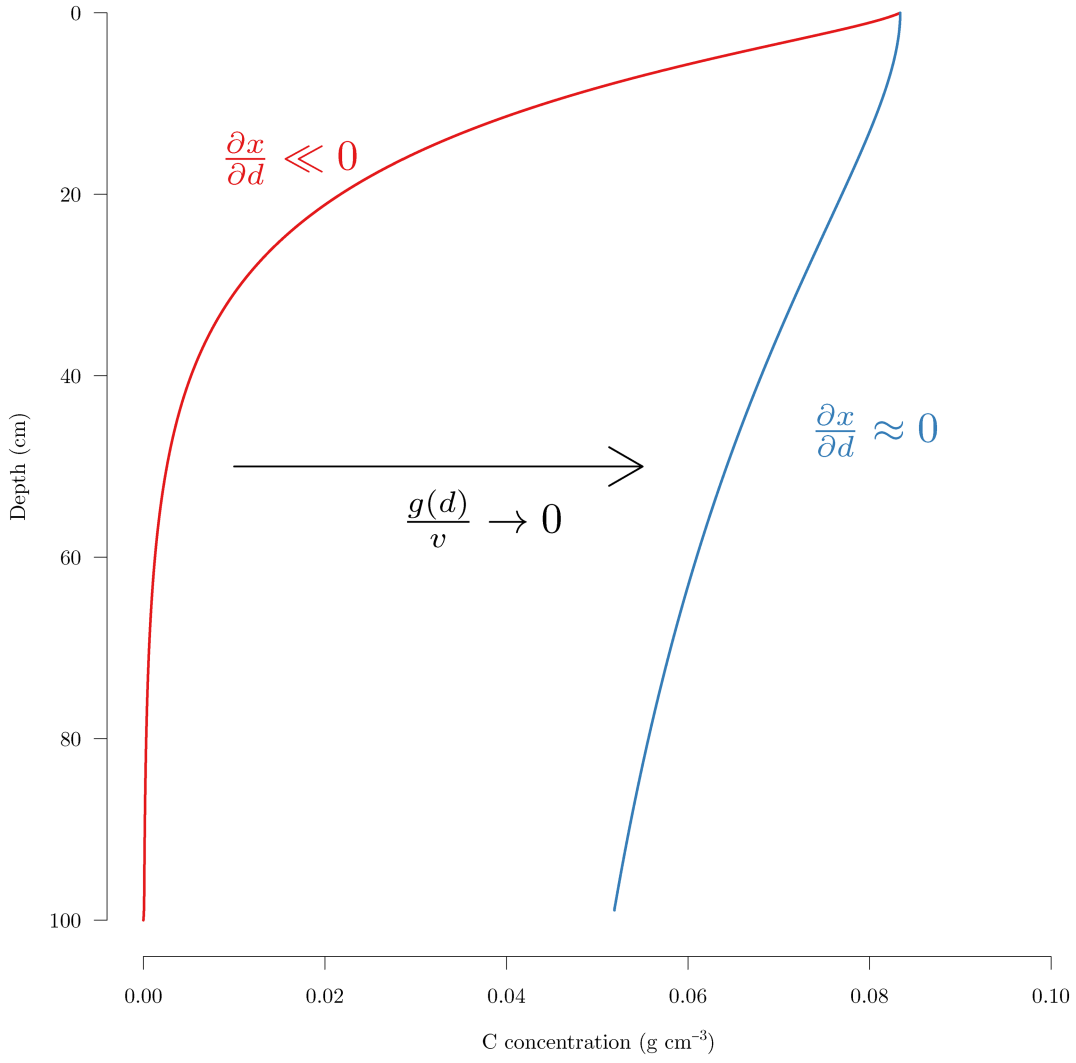

FIGURE 9 Graphical example for defining a management objective to increase C storage in the subsoil. By decreasing the ratio $g(d)/v$ as close to zero as possible, the decrease in C concentration with depth is less steep, and more carbon can be stored in the subsoil. For this example, advection velocity was increased from 1 to 100 cm year^{-1}.

decomposition. Equation (16) also suggests that a small difference between C inputs and decomposition across all depths [$g(d) \approx 0$] helps to decrease the gradient of C decline with depth. For example, exogenous amendments of organic matter with low decomposition rates could help to reduce this difference and reduce C decline with depth. There may be many other ways to achieve this management goal, and a challenge for future research would be to test this theoretical prediction through innovative experiments.

Equation (24) also suggests that changes in particle diffusion have little or no effect in contributing to increase carbon storage in the subsoil. This may imply that the diffusive mixing of carbon due to tillage plays no relevant role for increasing carbon in the entire profile.

7 | SUMMARY AND CONCLUSIONS

We reviewed the main processes that contribute to the formation of soil C profiles and the mathematical models that are used to represent them. Our main findings were: (1) The main processes that contribute to the formation of soil C profiles are root productivity and rhizodeposition, microbial decomposition, advective processes such as liquid phase transport, and diffusive processes such as bioturbation, cryoturbation, and tillage. (2) These processes can be expressed in models under the general paradigm of the diffusion–advection–reaction equation, with most previously proposed models being a special case of this general paradigm. (3) Advective and diffusive processes seem to be of secondary importance in explaining the shape of vertical soil C profiles. The difference between vertical carbon inputs and decomposition seems to play a primary role in explaining the decline of soil C with depth. (4) The transit time of C is only a few years to decades in most soils, which implies that promoting the addition of new C inputs to soils would only contribute to climate change mitigation in timescales of years to decades. CS at longer timescales is only possible in slow-cycling systems such as tundra and boreal forest soils, but primary production is relatively low in these regions. (5) Increasing C storage in the subsoil could be achieved by increasing rates of vertical transport through advective processes or by reducing the difference between plant inputs and decomposition at all depths, according to Equation (24). Innovative experiments and management practices are needed to test this prediction based on the current theoretical understanding of carbon dynamics in the subsoil.

Although soils store large quantities of C in the subsoil and this carbon is hundreds to thousands of years old, our review suggests that new carbon that enters the soil is cycled quickly by the activity of microorganisms with relatively fast transit times. Therefore, promoting new C inputs to subsoil may not have a significant contribution to climate change mitigation as it could be inferred from carbon stocks and ages in the subsoil alone. Conservation of existing subsoil C stocks seems to be a more relevant and important aspect because the timescales required to form existing soil C stocks were on the order of centuries to millenia, and there are important risks that, through land-use change or non-sustainable agricultural practices, important portions of these existing stocks may be lost quickly.

AUTHOR CONTRIBUTIONS

Carlos A. Sierra: Conceptualization; formal analysis; investigation; methodology; writing – original draft. **Bernhard Ahrens:** Writing – review and editing. **Martin A. Bolinder:** Writing – review and editing. **Maarten C. Braakhekke:** Writing – original draft. **Sophie von Fromm:** Data curation; formal analysis; visualization; writing – review and editing. **Thomas Kätterer:** Funding acquisition; writing – review and editing. **Zhongkui Luo:** Writing – review and editing. **Nargish Parvin:** Writing – review and editing. **Guocheng Wang:** Data curation; formal analysis; visualization; writing – review and editing.

ACKNOWLEDGMENTS

CAS would like to acknowledge financial support provided by the Faculty of Forest Sciences at the Swedish University of Agricultural Sciences and the Max Planck Society. SvF received funding from the International Max Planck Research School for Global Biogeochemical Cycles (IMPRS-gBGC). This study has also received funding from the European Unions' Horizon 2020 research and innovation programme under grant agreement No. 862695 EJP SOIL.

CONFLICT OF INTEREST STATEMENT

All authors declare no conflicts of interest.

DATA AVAILABILITY STATEMENT

All code and data required to reproduce the results of this manuscript are available at http://doi.org/10.5281/zenodo.10457957.

ORCID

Carlos A. Sierra https://orcid.org/0000-0003-0009-4169
Bernhard Ahrens https://orcid.org/0000-0001-7226-6682
Martin A. Bolinder https://orcid.org/0000-0002-3574-3061
Maarten C. Braakhekke https://orcid.org/0000-0002-1889-2225
Sophie von Fromm https://orcid.org/0000-0002-1820-1455
Thomas Kätterer https://orcid.org/0000-0002-1751-007X
Zhongkui Luo https://orcid.org/0000-0002-6744-6491
Nargish Parvin https://orcid.org/0000-0002-1571-575X
Guocheng Wang https://orcid.org/0000-0002-4141-4395

REFERENCES

Ahrens, B., Braakhekke, M. C., Guggenberger, G., Schrumpf, M., & Reichstein, M. (2015). Contribution of sorption, DOC transport and microbial interactions to the ^{14}C age of a soil organic carbon profile: Insights from a calibrated process model. *Soil Biology and Biochemistry*, *88*, 390–402.

Ahrens, B., Guggenberger, G., Rethemeyer, J., John, S., Marschner, B., Heinze, S., Angst, G., Mueller, C. W., Kögel-Knabner, I., Leuschner, C., Hertel, D., Bachmann, J., Reichstein, M., & Schrumpf, M. (2020). Combination of energy limitation and sorption capacity explains ^{14}C depth gradients. *Soil Biology and Biochemistry*, *148*, 107912.

Alcántara, V., Don, A., Well, R., & Nieder, R. (2016). Deep ploughing increases agricultural soil organic matter stocks. *Global Change Biology*, *22*(8), 2939–2956.

Allison, S. D., Wallenstein, M. D., & Bradford, M. A. (2010). Soil-carbon response to warming dependent on microbial physiology. *Nature Geoscience*, *3*(5), 336–340. https://doi.org/10.1038/ngeo846

Anderson, D. H. (2013). *Compartmental modeling and tracer kinetics* (Vol. *50*). Springer Science & Business Media.

Arndt, S., Jørgensen, B. B., LaRowe, D. E., Middelburg, J. J., Pancost, R. D., & Regnier, P. (2013). Quantifying the degradation of organic matter in marine sediments: A review and synthesis. *Earth-Science Reviews*, *123*, 53–86.

Baisden, W., & Parfitt, R. (2007). Bomb ^{14}C enrichment indicates decadal C pool in deep soil? *Biogeochemistry*, *85*(1), 59–68.

Baisden, W. T., Amundson, R., Brenner, D. L., Cook, A. C., Kendall, C., & Harden, J. W. (2002). A multiisotope C and N modeling analysis of soil organic matter turnover and transport as a function of soil depth in a California annual grassland soil chronosequence. *Global Biogeochemical Cycles*, *16*(4), 1135.

Balesdent, J., Basile-Doelsch, I., Chadoeuf, J., Cornu, S., Derrien, D., Fekiacova, Z., & Hatté, C. (2018). Atmosphere–soil carbon transfer as a function of soil depth. *Nature*, *559*(7715), 599–602.

Beck, H. E., Zimmermann, N. E., McVicar, T. R., Vergopolan, N., Berg, A., & Wood, E. F. (2018). Present and future Köppen-Geiger climate classification maps at 1-km resolution. *Scientific Data*, *5*(1), 180214.

Beer, C., Knoblauch, C., Hoyt, A. M., Hugelius, G., Palmtag, J., Mueller, C. W., & Trumbore, S. (2022). Vertical pattern of organic matter decomposability in cryoturbated permafrost-affected soils. *Environmental Research Letters*, *17*(10), 104023.

Bishop, T., McBratney, A., & Laslett, G. (1999). Modelling soil attribute depth functions with equal-area quadratic smoothing splines. *Geoderma*, *91*(1), 27–45.

Bockheim, J. G. (2007). Importance of cryoturbation in redistributing organic carbon in permafrost-affected soils. *Soil Science Society of America Journal*, *71*(4), 1335–1342.

Bolin, B., & Rodhe, H. (1973). A note on the concepts of age distribution and transit time in natural reservoirs. *Tellus*, *25*(1), 58–62.

Bolinder, M., Janzen, H., Gregorich, E., Angers, D., & VandenBygaart, A. (2007). An approach for estimating net primary productivity and annual carbon inputs to soil for common agricultural crops in Canada. *Agriculture, Ecosystems & Environment*, *118*(1), 29–42.

Bolinder, M. A., Crotty, F., Elsen, A., Frac, M., Kismányoky, T., Lipiec, J., Tits, M., Tóth, Z., & Kätterer, T. (2020). The effect of crop residues, cover crops, manures and nitrogen fertilization on soil organic carbon changes in agroecosystems: A synthesis of reviews. *Mitigation and Adaptation Strategies for Global Change*, *25*(6), 929–952.

Börjesson, G., Bolinder, M. A., Kirchmann, H., & Kätterer, T. (2018). Organic carbon stocks in topsoil and subsoil in long-term ley and cereal monoculture rotations. *Biology and Fertility of Soils*, *54*(4), 549–558.

Bosatta, E., & Ågren, G. I. (1996). Theoretical analyses of carbon and nutrient dynamics in soil profiles. *Soil Biology and Biochemistry*, *28*(10–11), 1523–1531.

Braakhekke, M. C., Beer, C., Hoosbeek, M. R., Reichstein, M., Kruijt, B., Schrumpf, M., & Kabat, P. (2011). Somprof: A vertically explicit soil organic matter model. *Ecological Modelling*, *222*(10), 1712–1730.

Braakhekke, M. C., Wutzler, T., Beer, C., Kattge, J., Schrumpf, M., Ahrens, B., Schöning, I., Hoosbeek, M. R., Kruijt, B., Kabat, P., & Reichstein, M. (2013). Modeling the vertical soil organic matter profile using Bayesian parameter estimation. *Biogeosciences*, *10*(1), 399–420.

Brovelli, A., Batlle-Aguilar, J., & Barry, D. (2012). Analysis of carbon and nitrogen dynamics in riparian soils: Model development. *Science of the Total Environment*, *429*, 231–245.

Bruun, S., Christensen, B. T., Thomsen, I. K., Jensen, E. S., & Jensen, L. S. (2007). Modeling vertical movement of organic matter in a soil incubated for 41 years with ^{14}C labeled straw. *Soil Biology and Biochemistry*, *39*(1), 368–371.

Bunzl, K. (2002). Transport of fallout radiocesium in the soil by bioturbation: A random walk model and application to a forest soil with a high abundance of earthworms. *Science of the Total Environment*, *293*(1), 191–200.

Button, E. S., Pett-Ridge, J., Murphy, D. V., Kuzyakov, Y., Chadwick, D. R., & Jones, D. L. (2022). Deep-C storage: Biological, chemical and physical strategies to enhance carbon stocks in agricultural subsoils. *Soil Biology and Biochemistry*, *170*, 108697.

Carter, M., & Gregorich, E. (2010). Carbon and nitrogen storage by deep-rooted tall fescue (*Lolium arundinaceum*) in the surface and subsurface soil of a fine sandy loam in eastern Canada. *Agriculture, Ecosystems & Environment*, *136*(1), 125–132.

Chabbi, A., Kögel-Knabner, I., & Rumpel, C. (2009). Stabilised carbon in subsoil horizons is located in spatially distinct parts of the soil profile. *Soil Biology and Biochemistry*, *41*(2), 256–261.

Chen, S., Martin, M. P., Saby, N. P., Walter, C., Angers, D. A., & Arrouays, D. (2018). Fine resolution map of top- and subsoil carbon sequestration potential in France. *Science of the Total Environment*, *630*, 389–400.

Chenu, C., Angers, D. A., Barré, P., Derrien, D., Arrouays, D., & Balesdent, J. (2019). Increasing organic stocks in agricultural soils: Knowledge gaps and potential innovations. *Soil and Tillage Research*, *188*, 41–52.

Collins, H., Smith, J., Fransen, S., Alva, A., Kruger, C., & Granatstein, D. (2010). Carbon sequestration under irrigated switchgrass (*Panicum virgatum* L.) production. *Soil Science Society of America Journal*, *74*(6), 2049–2058.

Cotrufo, M. F., & Lavallee, J. M. (2022). Soil organic matter formation, persistence, and functioning: A synthesis of current understanding to inform its conservation and regeneration. *Advances in Agronomy*, *172*, 1–66.

Crow, S., Reeves, M., Schubert, O., & Sierra, C. (2015). Optimization of method to quantify soil organic matter dynamics and carbon sequestration potential in volcanic ash soils. *Biogeochemistry*, *123*(1–2), 27–47.

Crow, S. E., & Sierra, C. A. (2022). The climate benefit of sequestration in soils for warming mitigation. *Biogeochemistry*, *161*, 71–84.

Dal Ferro, N., Piccoli, I., Berti, A., Polese, R., & Morari, F. (2020). Organic carbon storage potential in deep agricultural soil layers: Evidence from long-term experiments in northeast Italy. *Agriculture, Ecosystems & Environment*, *300*, 106967.

Don, A., Rödenbeck, C., & Gleixner, G. (2013). Unexpected control of soil carbon turnover by soil carbon concentration. *Environmental Chemistry Letters*, *11*, 407–413.

Dörr, H., & Münnich, K. O. (1989). Downward movement of soil organic matter and its influence on trace-element transport (^{210}Pb, ^{137}Cs) in the soil. *Radiocarbon*, *31*(3), 655–663.

Elzein, A., & Balesdent, J. (1995). Mechanistic simulation of vertical distribution of carbon concentrations and residence times in soils. *Soil Science Society of America Journal*, *59*(5), 1328–1335.

Eusterhues, K., Rumpel, C., Kleber, M., & Kögel-Knabner, I. (2003). Stabilisation of soil organic matter by interactions with minerals as revealed by mineral dissolution and oxidative degradation. *Organic Geochemistry*, *34*(12), 1591–1600.

Fan, J., McConkey, B., Wang, H., & Janzen, H. (2016). Root distribution by depth for temperate agricultural crops. *Field Crops Research*, *189*, 68–74.

Feng, X., Peterson, J. C., Quideau, S. A., Virginia, R. A., Graham, R. C., Sonder, L. J., & Chadwick, O. A. (1999). Distribution, accumulation, and fluxes of soil carbon in four monoculture lysimeters at San Dimas Experimental Forest, California. *Geochimica et Cosmochimica Acta*, *63*(9), 1319–1333.

Fey, M. V., & Schaetzl, R. J. (2017). Pedoturbation. In D. Richardson, N. Castree, M. F. Goodchild, A. Kobayashi, W. Liu, & R. A. Marston (Eds.), *International encyclopedia of geography* (pp. 1–11). John Wiley & Sons, Ltd.

Finke, P. A. (2012). Modeling the genesis of luvisols as a function of topographic position in loess parent material. *Quaternary International*, *265*, 3–17.

Freier, K. P., Glaser, B., & Zech, W. (2010). Mathematical modeling of soil carbon turnover in natural *Podocarpus* forest and *Eucalyptus* plantation in Ethiopia using compound specific $\delta^{13}C$ analysis. *Global Change Biology*, *16*(5), 1487–1502.

Gale, M. R., & Grigal, D. F. (1987). Vertical root distributions of northern tree species in relation to successional status. *Canadian Journal of Forest Research*, *17*(8), 829–834.

Georgiou, K., Jackson, R. B., Vindušková, O., Abramoff, R. Z., Ahlström, A., Feng, W., Harden, J. W., Pellegrini, A. F. A., Polley, H. W., Soong, J. L., Riley, W. J., & Torn, M. S. (2022). Global stocks and capacity of mineral-associated soil organic carbon. *Nature Communications*, *13*(1), 3797.

Gill, R. A., & Jackson, R. B. (2000). Global patterns of root turnover for terrestrial ecosystems. *New Phytologist*, *147*(1), 13–31.

Gjettermann, B., Styczen, M., Hansen, H. C. B., Vinther, F. P., & Hansen, S. (2008). Challenges in modelling dissolved organic matter dynamics in agricultural soil using daisy. *Soil Biology and Biochemistry*, *40*(6), 1506–1518.

Gleixner, G. (2013). Soil organic matter dynamics: A biological perspective derived from the use of compound-specific isotopes studies. *Ecological Research*, *28*(5), 683–695.

Grant, R., Juma, N., & McGill, W. (1993). Simulation of carbon and nitrogen transformations in soil: Mineralization. *Soil Biology and Biochemistry*, *25*(10), 1317–1329.

Guan, X.-K., Turner, N. C., Song, L., Gu, Y.-J., Wang, T.-C., & Li, F.-M. (2016). Soil carbon sequestration by three perennial legume pastures is greater in deeper soil layers than in the surface soil. *Biogeosciences*, *13*(2), 527–534.

Guenet, B., Eglin, T., Vasilyeva, N., Peylin, P., Ciais, P., & Chenu, C. (2013). The relative importance of decomposition and transport mechanisms in accounting for soil organic carbon profiles. *Biogeosciences*, *10*(4), 2379–2392.

Guo, L. B., & Gifford, R. M. (2002). Soil carbon stocks and land use change: A meta analysis. *Global Change Biology*, *8*(4), 345–360.

Guo, X., Mao, X., Yu, W., Xiao, L., Wang, M., Zhang, S., Zheng, J., Zhou, H., Luo, L., Chang, J., Shi, Z., & Luo, Z. (2023). A field incubation approach to evaluate the depth dependence of soil biogeochemical responses to climate change. *Global Change Biology*, *29*(3), 909–920.

Hansen, S., Jensen, H. E., Nielsen, N. E., & Svendsen, H. (1991). Simulation of nitrogen dynamics and biomass production in winter wheat using the danish simulation model daisy. *Fertilizer Research*, *27*(2), 245–259.

He, Y., Trumbore, S. E., Torn, M. S., Harden, J. W., Vaughn, L. J. S., Allison, S. D., & Randerson, J. T. (2016). Radiocarbon constraints imply reduced carbon uptake by soils during the 21st century. *Science*, *353*(6306), 1419–1424.

Heckman, K., Hicks Pries, C. E., Lawrence, C. R., Rasmussen, C., Crow, S. E., Hoyt, A. M., von Fromm, S. F., Shi, Z., Stoner, S., McGrath, C., Beem-Miller, J., Berhe, A. A., Blankinship, J. C., Keiluweit, M., Marín-Spiotta, E., Monroe, J. G., Plante, A. F., Schimel, J., Sierra, C. A., … Wagai, R. (2022). Beyond bulk: Density fractions explain heterogeneity in global soil carbon abundance and persistence. *Global Change Biology*, *28*(3), 1178–1196.

Hicks Pries, C., Ryals, R., Zhu, B., Min, K., Cooper, A., Goldsmith, S., Pett-Ridge, J., Torn, M., & Asefaw Berhe, A. (2023). The deep soil organic carbon response to global change. *Annual Review of Ecology, Evolution, and Systematics*, *54*(1), 375–401.

Hilbert, D. W., Roulet, N., & Moore, T. (2000). Modelling and analysis of peatlands as dynamical systems. *Journal of Ecology*, *88*(2), 230–242.

Hilinski, T. E. (2001). *Implementation of exponential depth distribution of organic carbon in the CENTURY model*. Department of Soil and Crop Sciences, Colorado State University.

Hinzmann, M., Ittner, S., Kiresiewa, Z., & Gerdes, H. (2021). An acceptance analysis of subsoil amelioration amongst agricultural actors in two regions in Germany. *Frontiers in Agronomy*, *3*, 660593.

Hole, F. D. (1961). A classification of pedoturbations and some other processes and factors of soil formation in relation to isotropism and anisotropism. *Soil Science*, *91*, 375–377.

Huang, Y., Lu, X., Shi, Z., Lawrence, D., Koven, C. D., Xia, J., Du, Z., Kluzek, E., & Luo, Y. (2018). Matrix approach to land carbon cycle modeling: A case study with the community land model. *Global Change Biology*, *24*(3), 1394–1404.

Jackson, R., Canadell, J., Ehleringer, J., Mooney, H., Sala, O., & Schulze, E. (1996). A global analysis of root distributions for terrestrial biomes. *Oecologia*, *10*, 389–411.

Jackson, R., Mooney, H., & Schulze, E.-D. (1997). A global budget for fine root biomass, surface area, and nutrient contents. *Proceedings of the National Academy of Sciences of the United States of America*, *94*, 7362–7366.

Jenkinson, D. S., & Coleman, K. (2008). The turnover of organic carbon in subsoils. Part 2. Modelling carbon turnover. *European Journal of Soil Science*, *59*(2), 400–413.

Jobbágy, E., & Jackson, R. (2000). The vertical distribution of soil organic carbon and its relation to climate and vegetation. *Ecological Applications*, *10*(2), 423–436.

Johnson, D. L., Watson-Stegner, D., Johnson, D. N., & Schaetzl, R. J. (1987). Proisotropic and proanisotropic processes of pedoturbation. *Soil Science*, *143*, 278–292.

Jordan, C. F., & Escalante, G. (1980). Root productivity in an Amazonian rain forest. *Ecology*, *61*(1), 14–18.

Kaiser, K., & Kalbitz, K. (2012). Cycling downwards – Dissolved organic matter in soils. *Soil Biology and Biochemistry*, *52*, 29–32.

Kalbitz, K., & Kaiser, K. (2008). Contribution of dissolved organic matter to carbon storage in forest mineral soils. *Journal of Plant Nutrition and Soil Science*, *171*(1), 52–60.

Kaste, J. M., Heimsath, A. M., & Bostick, B. C. (2007). Short-term soil mixing quantified with fallout radionuclides. *Geology*, *35*(3), 243–246.

Kätterer, T., Börjesson, G., & Kirchmann, H. (2014). Changes in organic carbon in topsoil and subsoil and microbial community composition caused by repeated additions of organic amendments and N fertilisation in a long-term field experiment in Sweden. *Agriculture, Ecosystems & Environment*, *189*, 110–118.

Kautz, T., Amelung, W., Ewert, F., Gaiser, T., Horn, R., Jahn, R., Javaux, M., Kemna, A., Kuzyakov, Y., Munch, J.-C., Pätzold, S., Peth, S., Scherer, H. W., Schloter, M., Schneider, H., Vanderborght, J., Vetterlein, D., Walter, A., Wiesenberg, G. L., & Köpke, U. (2013). Nutrient acquisition from arable subsoils in temperate climates: A review. *Soil Biology and Biochemistry*, *57*, 1003–1022.

Kell, D. B. (2011). Breeding crop plants with deep roots: Their role in sustainable carbon, nutrient and water sequestration. *Annals of Botany*, *108*(3), 407–418.

Keyvanshokouhi, S., Cornu, S., Lafolie, F., Balesdent, J., Guenet, B., Moitrier, N., Moitrier, N., Nougier, C., & Finke, P. (2019). Effects of soil process formalisms and forcing factors on simulated organic carbon depth-distributions in soils. *Science of the Total Environment*, *652*, 523–537.

Kindler, R., Siemens, J., Kaiser, K., Walmsley, D. C., Bernhofer, C., Buchmann, N., Cellier, P., Eugster, W., Gleixner, G., Grünwald, T., Heim, A., Ibrom, A., Jones, S. K., Jones, M., Klumpp, K., Kutsch, W., Larsen, K. S., Lehuger, S., Loubet, B., … Kaupenjohann, M. (2011). Dissolved carbon leaching from soil is a crucial component of the net ecosystem carbon balance. *Global Change Biology*, *17*(2), 1167–1185.

Kirchmann, H., Schön, M., Börjesson, G., Hamnér, K., & Kätterer, T. (2013). Properties of soils in the Swedish long-term fertility experiments: VII. Changes in topsoil and upper subsoil at Örja and Fors after 50 years of nitrogen fertilization and manure application. *Acta Agriculturae Scandinavica Section B Soil and Plant Science*, *63*(1), 25–36.

Kirkby, M. J. (1977). Soil development models as a component of slope models. *Earth Surface Processes*, *2*(2–3), 203–230.

Koven, C., Friedlingstein, P., Ciais, P., Khvorostyanov, D., Krinner, G., & Tarnocai, C. (2009). On the formation of high-latitude soil carbon stocks: Effects of cryoturbation and insulation by organic matter in a land surface model. *Geophysical Research Letters*, *36*(21), 40150.

Koven, C. D., Riley, W. J., Subin, Z. M., Tang, J. Y., Torn, M. S., Collins, W. D., Bonan, G. B., Lawrence, D. M., & Swenson, S. C. (2013). The effect of vertically resolved soil biogeochemistry and alternate soil C and N models on C dynamics of CLM4. *Biogeosciences*, *10*(11), 7109–7131.

Lanczos, C. (1996). *Linear differential operators*. Society for Industrial and Applied Mathematics.

Lawrence, C. R., Beem-Miller, J., Hoyt, A. M., Monroe, G., Sierra, C. A., Stoner, S., Heckman, K., Blankinship, J. C., Crow, S. E., McNicol, G., Trumbore, S., Levine, P. A., Vindušková, O., Todd-Brown, K., Rasmussen, C., Hicks Pries, C. E., Schädel, C., McFarlane, K., Doetterl, S., … Wagai, R. (2020). An open-source database for the synthesis of soil radiocarbon data: International Soil Radiocarbon Database (ISRaD) version 1.0. *Earth System Science Data*, *12*(1), 61–76.

LeVeque, R. J. (1990). *Numerical methods for conservation laws*. Birkhäuser Basel.

LeVeque, R. J. (2007). *Finite difference methods for ordinary and partial differential equations: Steady-state and time-dependent problems*. Society for Industrial and Applied Mathematics.

Li, C., Frolking, S., & Frolking, T. A. (1992). A model of nitrous oxide evolution from soil driven by rainfall events: 1. Model structure and sensitivity. *Journal of Geophysical Research: Atmospheres*, *97*(D9), 9759–9776.

Liang, J., Zhou, Z., Huo, C., Shi, Z., Cole, J. R., Huang, L., Konstantinidis, K. T., Li, X., Liu, B., Luo, Z., Penton, C. R., Schuur, E. A. G., Tiedje, J. M., Wang, Y.-P., Wu, L., Xia, J., Zhou, J., & Luo, Y. (2018). More replenishment than priming loss of soil organic carbon with additional carbon input. *Nature Communications*, *9*(1), 3175.

Liu, F., Wang, D., Zhang, B., & Huang, J. (2021). Concentration and biodegradability of dissolved organic carbon derived from soils: A global perspective. *Science of the Total Environment*, *754*, 142378.

Lorenz, K., & Lal, R. (2005). The depth distribution of soil organic carbon in relation to land use and management and the potential of carbon sequestration in subsoil horizons. *Advances in Agronomy*, *88*, 35–66.

Lu, X., Wang, Y.-P., Luo, Y., & Jiang, L. (2018). Ecosystem carbon transit versus turnover times in response to climate warming and rising atmospheric CO_2 concentration. *Biogeosciences*, *15*(21), 6559–6572.

Luo, Z., Luo, Y., Wang, G., Xia, J., & Peng, C. (2020). Warming-induced global soil carbon loss attenuated by downward carbon movement. *Global Change Biology*, *26*(12), 7242–7254.

Luo, Z., Wang, E., & Sun, O. J. (2010). Can no-tillage stimulate carbon sequestration in agricultural soils? A meta-analysis of paired experiments. *Agriculture, Ecosystems & Environment*, *139*(1), 224–231.

Manzoni, S., Katul, G. G., & Porporato, A. (2009). Analysis of soil carbon transit times and age distributions using network theories. *Journal of Geophysical Research*, *114*, 1070.

Manzoni, S., & Porporato, A. (2009). Soil carbon and nitrogen mineralization: Theory and models across scales. *Soil Biology and Biochemistry*, *41*(7), 1355–1379.

Marin-Spiotta, E., Chadwick, O. A., Kramer, M., & Carbone, M. S. (2011). Carbon delivery to deep mineral horizons in Hawaiian rain forest soils. *Journal of Geophysical Research: Biogeosciences*, *116*(G3), 1587.

Mary, B., Clivot, H., Blaszczyk, N., Labreuche, J., & Ferchaud, F. (2020). Soil carbon storage and mineralization rates are affected by carbon inputs rather than physical disturbance: Evidence from a 47-year tillage experiment. *Agriculture, Ecosystems & Environment*, *299*, 106972.

Mathieu, J. A., Hatté, C., Balesdent, J., & Parent, É. (2015). Deep soil carbon dynamics are driven more by soil type than by climate: A worldwide meta-analysis of radiocarbon profiles. *Global Change Biology*, *21*(11), 4278–4292.

Menichetti, L., Ekblad, A., & Kätterer, T. (2015). Contribution of roots and amendments to soil carbon accumulation within the soil profile in a long-term field experiment in Sweden. *Agriculture, Ecosystems & Environment*, *200*, 79–87.

Metzler, H., & Sierra, C. A. (2018). Linear autonomous compartmental models as continuous-time Markov chains: Transit-time and age distributions. *Mathematical Geosciences*, *50*(1), 1–34.

Metzler, H., Zhu, Q., Riley, W., Hoyt, A., Müller, M., & Sierra, C. A. (2020). Mathematical reconstruction of land carbon models from their numerical output: Computing soil radiocarbon from C dynamics. *Journal of Advances in Modeling Earth Systems*, *12*(1), e2019MS001776. https://doi.org/10.1029/2019MS001776

Michalzik, B., Kalbitz, K., Park, J. H., Solinger, S., & Matzner, E. (2001). Fluxes and concentrations of dissolved organic carbon and nitrogen – A synthesis for temperate forests. *Biogeochemistry*, *52*(2), 173–205.

Michalzik, B., Tipping, E., Mulder, J., Lancho, J. F. G., Matzner, E., Bryant, C. L., Clarke, N., Lofts, S., & Esteban, M. A. V. (2003). Modelling the production and transport of dissolved organic carbon in forest soils. *Biogeochemistry*, *66*(3), 241–264.

Morari, F., Berti, A., Dal Ferro, N., & Piccoli, I. (2019). *Deep carbon sequestration in cropping systems*. Springer International Publishing.

Mosier, S., Córdova, S. C., & Robertson, G. P. (2021). Restoring soil fertility on degraded lands to meet food, fuel, and climate security needs via perennialization. *Frontiers in Sustainable Food Systems*, *5*, 706142.

Moyano, F. E., Manzoni, S., & Chenu, C. (2013). Responses of soil heterotrophic respiration to moisture availability: An exploration of processes and models. *Soil Biology and Biochemistry*, *59*, 72–85.

Müller-Lemans, H., & van Dorp, F. (1996). Bioturbation as a mechanism for radionuclide transport in soil: Relevance of earthworms. *Journal of Environmental Radioactivity*, *31*(1), 7–20.

Nakane, K., & Shinozaki, K. (1978). A mathematical model of the behavior and vertical distribution of organic carbon in forest soils. *Japanese Journal of Ecology*, *28*(2), 111–122.

Neff, J. C., & Asner, G. P. (2001). Dissolved organic carbon in terrestrial ecosystems: Synthesis and a model. *Ecosystems*, *4*(1), 29–48.

O'Brien, B., & Stout, J. (1978). Movement and turnover of soil organic matter as indicated by carbon isotope measurements. *Soil Biology and Biochemistry*, *10*(4), 309–317.

Ota, M., Nagai, H., & Koarashi, J. (2013). Root and dissolved organic carbon controls on subsurface soil carbon dynamics: A model approach. *Journal of Geophysical Research: Biogeosciences*, *118*(4), 1646–1659.

Paustian, K., Lehmann, J., Ogle, S., Reay, D., Robertson, G. P., & Smith, P. (2016). Climate-smart soils. *Nature*, *532*(7597), 49–57.

Persson, T., Karlsson, P. S., Seyferth, U., Sjöberg, R. M., & Rudebeck, A. (2000). *Carbon mineralisation in European forest soils*. Springer.

Poeplau, C., & Don, A. (2013). Sensitivity of soil organic carbon stocks and fractions to different land-use changes across Europe. *Geoderma*, *192*, 189–201.

Ponce-Hernandez, R., Marriott, F. H. C., & Beckett, P. H. T. (1986). An improved method for reconstructing a soil profile from analyses of a small number of samples. *Journal of Soil Science*, *37*(3), 455–467.

Raich, J., & Nadelhoffer, K. (1989). Belowground carbon allocation in forest ecosystems: Global trends. *Ecology*, *70*(5), 1346–1354.

Rasmussen, C., Heckman, K., Wieder, W. R., Keiluweit, M., Lawrence, C. R., Berhe, A. A., Blankinship, J. C., Crow, S. E., Druhan, J. L., Hicks Pries, C. E., Marin-Spiotta, E., Plante, A. F., Schädel, C., Schimel, J. P., Sierra, C. A., Thompson, A., & Wagai, R. (2018). Beyond clay: Towards an improved set of variables for predicting soil organic matter content. *Biogeochemistry*, *137*(3), 297–306.

Rosenbloom, N. A., Doney, S. C., & Schimel, D. S. (2001). Geomorphic evolution of soil texture and organic matter in eroding landscapes. *Global Biogeochemical Cycles*, *15*(2), 365–381.

Roth, V.-N., Lange, M., Simon, C., Hertkorn, N., Bucher, S., Goodall, T., Griffiths, R. I., Mellado-Vázquez, P. G., Mommer, L., Oram, N. J., Weigelt, A., Dittmar, T., & Gleixner, G. (2019). Persistence of dissolved organic matter explained by molecular changes during its passage through soil. *Nature Geoscience*, *12*(9), 755–761.

Rumpel, C., Chabbi, A., & Marschner, B. (2012). *Carbon storage and sequestration in subsoil horizons: Knowledge, gaps and potentials*. Springer Netherlands.

Rumpel, C., & Kögel-Knabner, I. (2011). Deep soil organic matter—A key but poorly understood component of terrestrial C cycle. *Plant and Soil*, *338*(1), 143–158.

Salvador-Blanes, S., Minasny, B., & McBratney, A. B. (2007). Modelling long-term in situ soil profile evolution: Application to the genesis of soil profiles containing stone layers. *European Journal of Soil Science*, *58*(6), 1535–1548.

Sanderman, J., Hengl, T., & Fiske, G. J. (2017). Soil carbon debt of 12,000 years of human land use. *Proceedings of the National Academy of Sciences of the United States of America*, *114*(36), 9575–9580.

Sarmiento, J., & Gruber, N. (2006). *Ocean biogeochemical dynamics*. Princeton University Press.

Schaetzl, R. J., Burns, S. F., Small, T. W., & Johnson, D. L. (1990). Tree uprooting: Review of types and patterns of soil disturbance. *Physical Geography*, *11*(3), 277–291.

Scheibe, A., Sierra, C. A., & Spohn, M. (2023). Recently fixed carbon fuels microbial activity several meters below the soil surface. *Biogeosciences*, *20*(4), 827–838.

Schenk, H., & Jackson, R. (2002a). The global biogeography of roots. *Ecological Monographs*, *72*(3), 311–328.

Schenk, H., & Jackson, R. (2002b). Rooting depths, lateral root spreads and below-ground/above-ground allometries of plants in water limited ecosystem. *Journal of Ecology*, *90*, 480–494.

Schiedung, M., Tregurtha, C. S., Beare, M. H., Thomas, S. M., & Don, A. (2019). Deep soil flipping increases carbon stocks of New Zealand grasslands. *Global Change Biology*, *25*(7), 2296–2309.

Schimel, J. P., & Weintraub, M. N. (2003). The implications of exoenzyme activity on microbial carbon and nitrogen limitation in soil: A theoretical model. *Soil Biology and Biochemistry*, *35*(4), 549–563.

Shi, Z., Allison, S. D., He, Y., Levine, P. A., Hoyt, A. M., Beem-Miller, J., Zhu, Q., Wieder, W. R., Trumbore, S., & Randerson, J. T. (2020). The age distribution of global soil carbon inferred from radiocarbon measurements. *Nature Geoscience*, *13*(8), 555–559.

Sierra, C. A., Ceballos-Núñez, V., Metzler, H., & Müller, M. (2018). Representing and understanding the carbon cycle using the theory of compartmental dynamical systems. *Journal of Advances in Modeling Earth Systems*, *10*(8), 1729–1734.

Sierra, C. A., Crow, S. E., Heimann, M., Metzler, H., & Schulze, E.-D. (2021). The climate benefit of carbon sequestration. *Biogeosciences*, *18*(3), 1029–1048.

Sierra, C. A., Estupinan-Suarez, L. M., & Chanca, I. (2021). The fate and transit time of carbon in a tropical forest. *Journal of Ecology*, *109*(8), 2845–2855.

Sierra, C. A., Hoyt, A. M., He, Y., & Trumbore, S. E. (2018). Soil organic matter persistence as a stochastic process: Age and transit time distributions of carbon in soils. *Global Biogeochemical Cycles*, *32*(10), 1574–1588.

Sierra, C. A., & Müller, M. (2015). A general mathematical framework for representing soil organic matter dynamics. *Ecological Monographs*, *85*, 505–524.

Sierra, C. A., Müller, M., Metzler, H., Manzoni, S., & Trumbore, S. E. (2017). The muddle of ages, turnover, transit, and residence times in the carbon cycle. *Global Change Biology*, *23*(5), 1763–1773.

Sierra, C. A., Quetin, G. R., Metzler, H., & Müller, M. (2023). A decrease in the age of respired carbon from the terrestrial biosphere and increase in the asymmetry of its distribution. *Philosophical Transactions of the Royal Society A: Mathematical, Physical and Engineering Sciences*, *381*(2261), 20220200.

Sierra, C. A., Trumbore, S. E., Davidson, E. A., Vicca, S., & Janssens, I. (2015). Sensitivity of decomposition rates of soil organic matter with respect to simultaneous changes in temperature and moisture. *Journal of Advances in Modeling Earth Systems*, *7*(1), 335–356.

Slessarev, E. W., Nuccio, E. E., McFarlane, K. J., Ramon, C. E., Saha, M., Firestone, M. K., & Pett-Ridge, J. (2020). Quantifying the effects of switchgrass (*Panicum virgatum*) on deep organic C stocks using natural abundance ^{14}C in three marginal soils. *GCB Bioenergy*, *12*(10), 834–847.

Taghizadeh-Toosi, A., Christensen, B. T., Hutchings, N. J., Vejlin, J., Kätterer, T., Glendining, M., & Olesen, J. E. (2014). C-tool: A simple model for simulating whole-profile carbon storage in temperate agricultural soils. *Ecological Modelling*, *292*, 11–25.

Tao, F., Huang, Y., Hungate, B. A., Manzoni, S., Frey, S. D., Schmidt, M. W. I., Reichstein, M., Carvalhais, N., Ciais, P., Jiang, L., Lehmann, J., Wang, Y.-P., Houlton, B. Z., Ahrens, B., Mishra, U., Hugelius, G., Hocking, T. D., Lu, X., Shi, Z., … Luo, Y. (2023). Microbial carbon use efficiency promotes global soil carbon storage. *Nature*, *618*(7967), 981–985.

Thompson, M. V., & Randerson, J. T. (1999). Impulse response functions of terrestrial carbon cycle models: Method and application. *Global Change Biology*, *5*(4), 371–394. https://doi.org/10.1046/j.1365-2486.1999.00235.x

Thorup-Kristensen, K., Halberg, N., Nicolaisen, M., Olesen, J. E., Crews, T. E., Hinsinger, P., Kirkegaard, J., Pierret, A., & Dresbøll, D. B. (2020). Digging deeper for agricultural resources, the value of deep rooting. *Trends in Plant Science*, *25*(4), 406–417.

Tifafi, M., Camino-Serrano, M., Hatté, C., Morras, H., Moretti, L., Barbaro, S., Cornu, S., & Guenet, B. (2018). The use of radiocarbon ^{14}C to constrain carbon dynamics in the soil module of the land surface model ORCHIDEE (SVN r5165). *Geoscientific Model Development*, *11*(12), 4711–4726.

van Dam, D., van Breemen, N., & Veldkamp, E. (1997). Soil organic carbon dynamics: Variability with depth in forested and deforested soils under pasture in Costa Rica. *Biogeochemistry*, *39*(3), 343–375.

van Veen, J. A., & Paul, E. A. (1981). Organic carbon dynamics in grassland soils. 1. Background information and computer simulation. *Canadian Journal of Soil Science*, *61*(2), 185–201.

VandenBygaart, A. J., Bremer, E., McConkey, B. G., Ellert, B. H., Janzen, H. H., Angers, D. A., Carter, M. R., Drury, C. F., Lafond, G. P., & McKenzie, R. H. (2011). Impact of sampling depth on differences in soil carbon stocks in long-term agroecosystem experiments. *Soil Science Society of America Journal*, *75*(1), 226–234.

Wang, G., Xiao, L., Lin, Z., Zhang, Q., Guo, X., Cowie, A., Zhang, S., Wang, M., Chen, S., Zhang, G., Shi, Z., Sun, W., & Luo, Z. (2023). Most root-derived carbon inputs do not contribute to long-term global soil carbon storage. *Science China Earth Sciences*, *66*(5), 1072–1086.

Wang, X., Xu, X., Qiu, S., Zhao, S., & He, P. (2023). Deep tillage enhanced soil organic carbon sequestration in China: A meta-analysis. *Journal of Cleaner Production*, *399*, 136686.

Wang, Y.-P., Zhang, H., Ciais, P., Goll, D., Huang, Y., Wood, J. D., Ollinger, S. V., Tang, X., & Prescher, A.-K. (2021). Microbial activity and root carbon inputs are more important than soil carbon diffusion

in simulating soil carbon profiles. *Journal of Geophysical Research: Biogeosciences*, *126*(4), e2020JG006205.

Xiao, L., Wang, G., Chang, J., Chen, Y., Guo, X., Mao, X., Wang, M., Zhang, S., Shi, Z., Luo, Y., Cheng, L., Yu, K., Mo, F., & Luo, Z. (2023). Global depth distribution of belowground net primary productivity and its drivers. *Global Ecology and Biogeography*, *32*(8), 1435–1451.

Xiao, L., Wang, G., Wang, M., Zhang, S., Sierra, C. A., Guo, X., Chang, J., Shi, Z., & Luo, Z. (2022). Younger carbon dominates global soil carbon efflux. *Global Change Biology*, *28*(18), 5587–5599.

How to cite this article: Sierra, C. A., Ahrens, B., Bolinder, M. A., Braakhekke, M. C., von Fromm, S., Kätterer, T., Luo, Z., Parvin, N., & Wang, G. (2024). Carbon sequestration in the subsoil and the time required to stabilize carbon for climate change mitigation. *Global Change Biology*, *30*, e17153. https://doi.org/10.1111/gcb.17153